

A unified computational framework for bulk and surface elasticity theory: a curvilinear-coordinate-based finite element methodology

A. Javili · A. McBride · P. Steinmann · B. D. Reddy

Received: 2 December 2013 / Accepted: 3 April 2014 / Published online: 1 May 2014
© Springer-Verlag Berlin Heidelberg 2014

Abstract A curvilinear-coordinate-based finite element methodology is presented as a basis for a straightforward computational implementation of the theory of surface elasticity that mimics the underlying mathematical and geometrical concepts. An efficient formulation is obtained by adopting the same methodology for both the bulk and the surface. The key steps to evaluate the hyperelastic constitutive relations at the level of the quadrature point in a finite element scheme using this unified approach are provided. The methodology is illustrated through selected numerical examples.

Keyword Surface elasticity · Curvilinear coordinates · Finite element

1 Introduction

The surface elasticity theory of Gurtin and Murdoch [21] and variants thereof have been applied to study the mechanical response of micro- and nanoscale solids. Integral to the theory is the derivation of a set of governing equations and constitutive relations that describe the behaviour of the surface of the bulk object. Earlier related contributions include

those by Scriven [43] on the dynamics of fluid interfaces. Scriven employed many of the fundamental concepts formalised by Gurtin and Murdoch [21], including the use of the term *surface elasticity* [44]. The study of the behaviour of fluid surfaces dates back to the work, primarily on the capillary effect, of Laplace, Young and Gibbs. For extensive reviews of surface elasticity see [15,28].

The role of surface (interface) elasticity and the size-dependence of the elastic response has received considerable attention recently (see e.g. [6,16–18,25,35,45–47,55,59]). This resurgence of interest in the mechanics of solid surfaces can be largely attributed to the increasing number of applications involving nanoscale structures. In such applications the surface-to-volume ratio becomes significant (see e.g. the seminal works [24,38,49]). Relevant works include those by Cammarata [8] who detailed the role of the surface and interface stress in the thermodynamics of solids and provided some experimental measurements at the nanoscale to underpin the theory. Miller and Shenoy [37] compared the surface elasticity model with direct atomistic simulations of nanoscale structures using the embedded atom method. They showed very good agreement between the atomistic simulations and the continuum model. Dingreville et al. [14] proposed a framework to incorporate the surface free energy into the theory of continuum mechanics. They demonstrated that surface effects become significant when at least one of the dimensions of the problem is in the nanometer range. The influence of the surface on the elastic behaviour of nanowires in static bending was investigated by He and Lilley [22] using the Young–Laplace equation. Hung and Wang [26] and Wang et al. [53] proposed a theory of hyperelasticity accounting for surface energy effects and showed how surface tension induces a residual stress field in the bulk of nanostructures. Park and Klein [39,40], Park et al. [41] developed an alternative continuum framework, based on the surface Cauchy–

A. Javili (✉) · P. Steinmann
Chair of Applied Mechanics, University of Erlangen–Nuremberg,
Egerlandstr. 5, 91058 Erlangen, Germany
e-mail: ali.javili@ltm.uni-erlangen.de

P. Steinmann
e-mail: paul.steinmann@ltm.uni-erlangen.de

A. McBride · B. D. Reddy
Centre for Research in Computational and Applied Mechanics,
University of Cape Town, Rondebosch 7701, South Africa
e-mail: andrew.mcbride@uct.ac.za

B. D. Reddy
e-mail: daya.reddy@uct.ac.za

Born model, to include surface stresses. Wei et al. [54] studied the size-dependent mechanical properties of nanostructures with the finite element method in two dimensions. Size effects observed in ZnO nanowires have been studied using surface elasticity theory [1, 58].

Contributions by some of the authors of this work include the development of a finite-element framework for continua with elastic boundary surfaces [30, 31]. The framework is based on finite-strain theory and inherently accounts for geometrical nonlinearities and surface anisotropy. These contributions do not, however, exploit fully the powerful curvilinear-coordinate framework, nor do they provide details of the algorithm to compute the constitutive response at the level of the quadrature point. The theory of thermoelasticity at the nanoscale is elaborated upon in [32, 33]. Javili et al. [29] study the admissible range for the surface material parameters. In particular, the validity of negative surface parameters, which have been reported in the literature, is assessed.

It is clear from the significant body of work on surface elasticity that a robust computational framework is required to solve the more challenging problems involving, for example, finite deformations and surface tension. Such a computational framework is the primary objective of this work. A novel curvilinear-coordinate-based finite element methodology is presented. The primary advantages of the methodology are, first, that it allows for a straightforward computational implementation of the theory of surface elasticity that mimics the underlying mathematical and geometrical concepts, and, second, that it naturally accommodates curved surfaces. Similar approaches have been adopted in shell theory (see e.g. Wriggers [56] and the reference therein). In related works, [2] applied the theory of elasticity with surface stresses to the modelling of shells with nanoscale thickness. Steigmann [50] demonstrated how membrane theory can be regarded as a special case of the Cosserat theory of elastic surfaces, or, alternatively, derived from three-dimensional elasticity theory via asymptotic or variational methods (see also, [5, 20]). Perić and colleagues [12, 42] carried out the finite element implementations accounting for surface tension in fluids (see also [51] in the context of heat conduction).

An efficient formulation is obtained here by adopting the same methodology for both the bulk and the surface. The use of such a formulation in the absence of surface effects hold no obvious advantage over the conventional approach, and we have not seen mention of any such approach in the finite element literature. However, for problems in surface elasticity it is clearly advantageous. The key steps to evaluate the hyperelastic constitutive relations at the level of the quadrature point in a finite element scheme using this unified approach are provided. In particular, we detail the computation of the inverse of the rank-deficient surface deformation gradient. The complete, documented code used to generate the numer-

ical examples presented here is available and described in a companion paper [36].¹

Section 2 summarizes the key concepts required from differential geometry. The problem of surface elasticity is defined and constitutive relations discussed. The key steps in the numerical implementation using the finite element method are given in Sect. 3. Finally, a series of numerical examples is presented in Sect. 4.

2 Theory

The objective of this section is to present theoretical aspects of a unified framework to study both bulk and surface elasticity theories. The required notation and definitions are first introduced. Thereafter, Sect. 2.2 briefly reviews results in differential geometry required to describe the kinematics of the bulk and the surface. Although the results for the bulk are standard, they clarify, in a familiar framework, the results on the surface. Both sets of results are presented as a foundation for the unified framework proposed in Sect. 2.3. Further details on differential geometry can be found in [9, 19, 34] among many others. The problem of interest is introduced in Sect. 2.3 and the kinematics and various underlying assumptions are discussed. The governing equations are also given. A nonlinear hyperelastic material model for the bulk together with its associated stress and tangent are given in Sect. 2.5. The vast majority of the surface elasticity models in the literature are based upon the infinitesimal theory. Here, the surface is modelled using an isotropic hyperelastic model. It is demonstrated how linearization of the current model leads to the classical linear one.

2.1 Notation and definitions

Direct notation is adopted throughout. Occasional use is made of index notation, the summation convention for repeated indices being implied. When the repeated indices are lower-case italic letters the summation is over the range $\{1, 2, 3\}$. If they are lower-case Greek letters the summation is over the range $\{1, 2\}$. Three-dimensional Euclidean space is denoted \mathbf{E}^3 . The scalar product of two vectors \mathbf{a} and \mathbf{b} is denoted $\mathbf{a} \cdot \mathbf{b} = [\mathbf{a}]^i [\mathbf{b}]_i$ where $[\mathbf{a}]^i$ and $[\mathbf{b}]_i$ are the contravariant components of the vector \mathbf{a} and covariant components of the vector \mathbf{b} , respectively. The scalar product of two second-order tensors \mathbf{A} and \mathbf{B} is denoted $\mathbf{A} : \mathbf{B} = [\mathbf{A}]^{ij} [\mathbf{B}]_{ij}$. The composition of two second-order tensors \mathbf{A} and \mathbf{B} , denoted $\mathbf{A} \cdot \mathbf{B}$, is a second-order tensor with components $[\mathbf{A} \cdot \mathbf{B}]_{ij} = [\mathbf{A}]_i^m [\mathbf{B}]_{mj}$. The action of a second-order tensor \mathbf{A} on a vector \mathbf{a} is given by $[\mathbf{A} \cdot \mathbf{a}]_i = [\mathbf{A}]_i^j [\mathbf{a}]_j$.

¹ The documented program can be found at http://www.cerecam.uct.ac.za/code/surface_energy/doc/html/.

Fig. 1 Illustration of the Cartesian basis \mathcal{E} and an arbitrary basis \mathcal{G} along with its dual basis

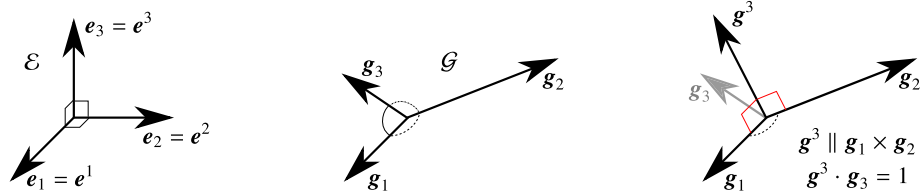
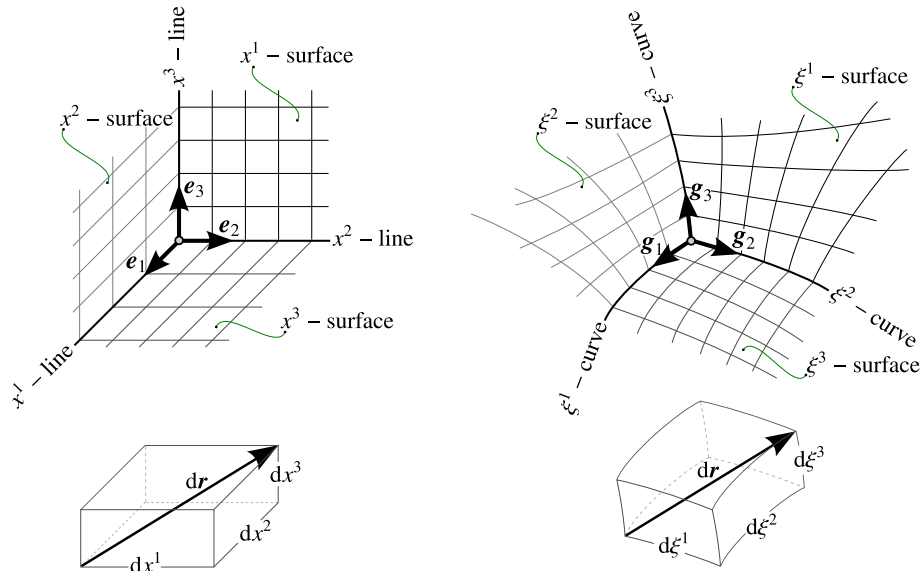


Fig. 2 Illustration of the Cartesian coordinate system and a general curvilinear coordinate system. An arbitrary infinitesimal vector $d\mathbf{r}$ is shown in both coordinate systems



The tensor product of two vectors \mathbf{a} and \mathbf{b} is a second-order tensor $\mathbf{D} = \mathbf{a} \otimes \mathbf{b}$ with $[D]_{ij} = [a]_i [b]_j$. The two non-standard tensor products of two second-order tensors \mathbf{A} and \mathbf{B} are the fourth-order tensors $[\mathbf{A} \otimes \mathbf{B}]_{ijkl} = [\mathbf{A}]_{ik} [\mathbf{B}]_{jl}$ and $[\mathbf{A} \underline{\otimes} \mathbf{B}]_{ijkl} = [\mathbf{A}]_{il} [\mathbf{B}]_{jk}$.

An arbitrary quantity in the bulk is denoted $\{\bullet\}$ and analogously $\{\bullet\}$ denotes an arbitrary surface quantity. The surface quantity can be a vector, not necessarily tangent to the surface, or a tensor, not necessarily tangential or superficial to the surface. In Sect. 2.2 all quantities and operators are denoted by small letters. In Sect. 2.3 and what follows, we distinguish between quantities in the material and spatial configurations using upper- and lower-case letters, respectively. The (conventional) identity tensor in \mathbf{E}^3 is denoted as \mathbf{i} . The degeneration of the three-dimensional identity to the two-dimensional space is defined by \mathbf{i}_2 .

2.2 Key concepts in differential geometry

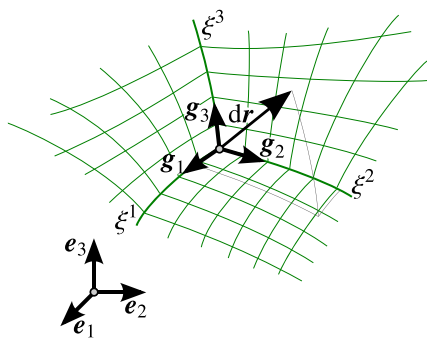
Let \mathcal{E} denote the Cartesian (standard-orthonormal) basis in \mathbf{E}^3 , as shown in Fig. 1, with unit basis vectors $\mathbf{e}_i = \mathbf{e}^i$ and $\mathbf{e}_i \cdot \mathbf{e}_j = \delta_{ij}$. The indices i and j run from 1 to 3 and $\delta_{ij} = \delta_i^j$ denotes the Kronecker delta, i.e. $\mathcal{E} = \{\mathbf{e}_1, \mathbf{e}_2, \mathbf{e}_3\} = \{\mathbf{e}^1, \mathbf{e}^2, \mathbf{e}^3\}$. Let $\mathcal{G} = \{\mathbf{g}_1, \mathbf{g}_2, \mathbf{g}_3\}$ be an arbitrary basis in \mathbf{E}^3 , see Fig. 1. The basis $\mathcal{G}^* = \{\mathbf{g}^1, \mathbf{g}^2, \mathbf{g}^3\}$ is the dual to \mathcal{G} , and vice versa, if and only if $\mathbf{g}_i \cdot \mathbf{g}^j = \delta_i^j$ for all i and j . It can

be shown that for a given basis \mathcal{G} , its dual basis \mathcal{G}^* always exists, is unique and forms a basis in \mathbf{E}^3 see e.g. [27].

Figure 2 illustrates the Cartesian coordinate system and a general curvilinear coordinate system. Let $d\mathbf{r}$ denote an arbitrary infinitesimal vector expressed in terms of the Cartesian coordinates as shown in Fig. 2(left). The vector $d\mathbf{r}$ can be expressed in terms of curvilinear coordinates ξ^i as shown in Fig. 2(right). This straightforward coordinate transformation is performed by expressing the Cartesian basis in terms of the curvilinear one as follows: $\mathbf{e}_i = \alpha_i^j \mathbf{g}_j$ where α_i^j are the nine coefficients required to linearly map the two coordinates. Clearly the mapping of the coordinates is invertible. One can express the curvilinear basis in terms of the Cartesian one as $\mathbf{g}_i = \beta_i^j \mathbf{e}_j$ with β_i^j the linear mapping from the curvilinear coordinates to the Cartesian ones which is inverse to α_i^j , i.e. $[\beta_i^j] = [\alpha_i^j]^{-1}$. Let g^{ij} denote the mapping from the contravariant basis to the covariant one, and g_{ij} the mapping from the covariant basis to the contravariant one; that is:

$$\mathbf{g}^i = g^{ij} \mathbf{g}_j \quad \text{and} \quad \mathbf{g}_i = g_{ij} \mathbf{g}^j.$$

It can be proven that these two mappings are inverse to each other, i.e. $[g_{ij}] = [g^{ij}]^{-1}$. Furthermore the coefficients are found from $g_{ij} = \mathbf{g}_i \cdot \mathbf{g}_j$ and $g^{ij} = \mathbf{g}^i \cdot \mathbf{g}^j$. The coefficients g_{ij} and g^{ij} are termed the covariant and contravariant metric coefficients, respectively. The covariant metric is denoted as

Table 1 The key differential geometry concepts in the bulk

$$d\mathbf{r} = d\mathbf{r}(\xi) = d\mathbf{r}(\xi^1, \xi^2, \xi^3)$$

$$\mathbf{g}_i = \frac{\partial \mathbf{r}}{\partial \xi^i}, \quad \mathbf{g}^i = \frac{\partial \xi^i}{\partial \mathbf{r}} \quad \text{with} \quad i, j \in \{1, 2, 3\}$$

$$\text{grad}\{\bullet\} = \frac{\partial \{\bullet\}}{\partial \xi^i} \otimes \mathbf{g}_i, \quad \text{div}\{\bullet\} = \frac{\partial \{\bullet\}}{\partial \xi^i} \cdot \mathbf{g}_i = \text{grad}\{\bullet\} : \mathbf{i}$$

$$\det\{\bullet\} = \frac{[\{\bullet\} \cdot \mathbf{g}_1] \cdot [[\{\bullet\} \cdot \mathbf{g}_2] \times [\{\bullet\} \cdot \mathbf{g}_3]]}{\mathbf{g}_1 \cdot [\mathbf{g}_2 \times \mathbf{g}_3]}$$

$$\mathbf{g}_i = g_{ij} \mathbf{g}^j, \quad g_{ij} = \mathbf{g}_i \cdot \mathbf{g}_j, \quad \mathbf{g}^i = g^{ij} \mathbf{g}_j, \quad g^{ij} = \mathbf{g}^i \cdot \mathbf{g}^j, \quad [g_{ij}] = [g^{ij}]^{-1}, \quad g = |[g_{ij}]|$$

$$\mathfrak{g} : \text{permutation tensor}, \quad \mathfrak{g} = g_{rst} \mathbf{g}^r \otimes \mathbf{g}^s \otimes \mathbf{g}^t = g^{rst} \mathbf{g}_r \otimes \mathbf{g}_s \otimes \mathbf{g}_t, \quad g_{rst} = g^{rst} g = \sqrt{g} e_{rst}$$

$$g_{rst} = g^{rst} g = \begin{cases} \sqrt{g} & \text{if } rst \text{ is an even permutation of } 123 \\ -\sqrt{g} & \text{if } rst \text{ is an odd permutation of } 123 \\ 0 & \text{otherwise} \end{cases}, \quad e_{rst} = \begin{cases} 1 & \text{if } rst \text{ is an even permutation of } 123 \\ -1 & \text{if } rst \text{ is an odd permutation of } 123 \\ 0 & \text{otherwise} \end{cases}$$

$$g_{rst} = \mathbf{g}_r \cdot [\mathbf{g}_s \times \mathbf{g}_t], \quad g^{rst} = \mathbf{g}^r \cdot [\mathbf{g}^s \times \mathbf{g}^t]$$

$$\mathbf{u} \times \mathbf{v} = [\mathbf{u} \otimes \mathbf{v}] : \mathfrak{g}, \quad \mathbf{u} \cdot \mathbf{v} = [\mathbf{u} \otimes \mathbf{v}] : \mathbf{i}, \quad \mathbf{i} = \delta_j^i \mathbf{g}_i \otimes \mathbf{g}^j = \mathbf{g}_i \otimes \mathbf{g}^i = \mathbf{g}_1 \otimes \mathbf{g}^1 + \mathbf{g}_2 \otimes \mathbf{g}^2 + \mathbf{g}_3 \otimes \mathbf{g}^3$$

g and is defined as the determinant of the matrix of covariant metric coefficients, i.e. $g = |[g_{ij}]|$. The contravariant metric g^{-1} is the determinant of the matrix of contravariant metric coefficients. The gradient, divergence and determinant operators in a general curvilinear coordinates as applied to tensors are defined as follows:

$$\text{grad}\{\bullet\} = \frac{\partial \{\bullet\}}{\partial \xi^i} \otimes \mathbf{g}_i$$

$$\text{div}\{\bullet\} = \frac{\partial \{\bullet\}}{\partial \xi^i} \cdot \mathbf{g}_i = \text{grad}\{\bullet\} : \mathbf{i}$$

$$\det\{\bullet\} = \frac{[\{\bullet\} \cdot \mathbf{g}_1] \cdot [[\{\bullet\} \cdot \mathbf{g}_2] \times [\{\bullet\} \cdot \mathbf{g}_3]]}{\mathbf{g}_1 \cdot [\mathbf{g}_2 \times \mathbf{g}_3]}.$$

The main concepts and definitions pertaining to the differential geometry of the bulk are gathered in Table 1.

A two-dimensional (smooth) surface \mathcal{S} in E^3 can be parametrized by two surface coordinates $\hat{\xi}^1$ and $\hat{\xi}^2$. The corresponding tangent vectors to the surface coordinate lines $\hat{\xi}^\alpha$, i.e. the covariant (natural) surface basis vectors, are given by $\hat{\mathbf{g}}_\alpha = \partial \mathbf{r} / \partial \hat{\xi}^\alpha$. The associated contravariant (dual) surface basis vectors are denoted as $\hat{\mathbf{g}}^\alpha$ in analogy to the bulk and are related to the covariant surface basis vectors by the co- and contravariant surface metric coefficients (first fundamental form for the surface) as

$$\hat{\mathbf{g}}^\alpha = \hat{\mathbf{g}}^{\alpha\beta} \hat{\mathbf{g}}_\beta \quad \text{and} \quad \hat{\mathbf{g}}_\alpha = \hat{\mathbf{g}}_{\alpha\beta} \hat{\mathbf{g}}^\beta.$$

In a near-identical fashion to the bulk, it can be shown that the two metrics are inverse to each other, i.e. $[\hat{\mathbf{g}}_{\alpha\beta}] = [\hat{\mathbf{g}}^{\alpha\beta}]^{-1}$ and furthermore the coefficients are $\hat{\mathbf{g}}_{\alpha\beta} = \hat{\mathbf{g}}_\alpha \cdot \hat{\mathbf{g}}_\beta$ and $\hat{\mathbf{g}}^{\alpha\beta} = \hat{\mathbf{g}}^\alpha \cdot \hat{\mathbf{g}}^\beta$. The contra- and covariant base vectors $\hat{\mathbf{g}}^3$ and $\hat{\mathbf{g}}_3$, normal to the surface, are defined by $\hat{\mathbf{g}}^3 = \hat{\mathbf{g}}_1 \times \hat{\mathbf{g}}_2$ and $\hat{\mathbf{g}}_3 = [\hat{\mathbf{g}}^{33}]^{-1} \hat{\mathbf{g}}^3$ such that $\hat{\mathbf{g}}_3 \cdot \hat{\mathbf{g}}^3 = 1$. The unit normal to the surface \mathbf{n} is parallel to $\hat{\mathbf{g}}_3$ and $\hat{\mathbf{g}}^3$ and can be calculated as $\mathbf{n} = \hat{\mathbf{g}}_3 / |\hat{\mathbf{g}}_3| = \hat{\mathbf{g}}^3 / |\hat{\mathbf{g}}^3|$. The surface identity tensor is defined as $\hat{\mathbf{i}} = \mathbf{i} - \hat{\mathbf{g}}_3 \otimes \hat{\mathbf{g}}^3 = \mathbf{i} - \mathbf{n} \otimes \mathbf{n}$. The surface gradient, divergence and determinant operators in a general curvilinear coordinates are defined as

$$\widehat{\text{grad}}\{\bullet\} = \frac{\partial \{\bullet\}}{\partial \hat{\xi}^\alpha} \otimes \hat{\mathbf{g}}_\alpha$$

$$\widehat{\text{div}}\{\bullet\} = \frac{\partial \{\bullet\}}{\partial \hat{\xi}^\alpha} \cdot \hat{\mathbf{g}}_\alpha = \widehat{\text{grad}}\{\bullet\} : \hat{\mathbf{i}}$$

$$\widehat{\det}\{\bullet\} = \frac{[[\{\bullet\} \cdot \hat{\mathbf{g}}_1] \times [\{\bullet\} \cdot \hat{\mathbf{g}}_2]]}{|\hat{\mathbf{g}}_1 \times \hat{\mathbf{g}}_2|}.$$

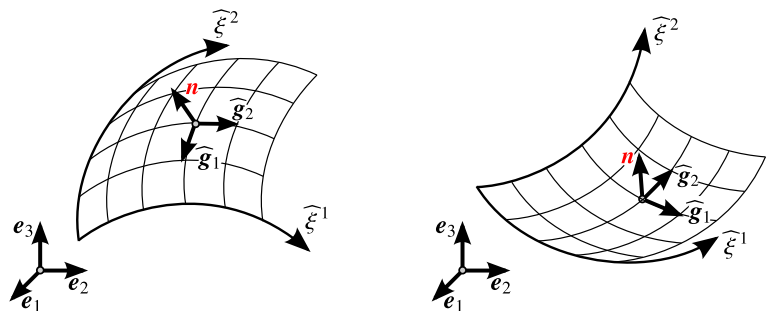
The main concepts and definitions for the differential geometry of the surface are gathered in Table 2.

Remark Surface curvature The surface curvature tensor $\hat{\kappa}$ is defined as the negative surface gradient of the normal \mathbf{n} , i.e.

Table 2 The key differential geometry concepts of the surface

	$dr = d\mathbf{r}(\xi) = d\mathbf{r}(\xi^1, \xi^2)$ $\widehat{\mathbf{g}}_\alpha = \frac{\partial \mathbf{r}}{\partial \xi^\alpha} \quad , \quad \widehat{\mathbf{g}}^\alpha = \frac{\partial \xi^\alpha}{\partial \mathbf{r}} \quad \text{with} \quad \alpha, \beta \in \{1, 2\}$ $\widehat{\mathbf{g}}^3 = \widehat{\mathbf{g}}_1 \times \widehat{\mathbf{g}}_2 \quad , \quad \widehat{\mathbf{g}}_3 = [\widehat{\mathbf{g}}^{33}]^{-1} \widehat{\mathbf{g}}^3 \quad , \quad \mathbf{n} = \sqrt{\widehat{\mathbf{g}}_{33}} \widehat{\mathbf{g}}^3 = \sqrt{\widehat{\mathbf{g}}^{33}} \widehat{\mathbf{g}}_3$ $\widehat{\text{grad}}\{\bullet\} = \frac{\partial \{\bullet\}}{\partial \xi^\alpha} \otimes \widehat{\mathbf{g}}_\alpha \quad , \quad \widehat{\text{div}}\{\bullet\} = \frac{\partial \{\bullet\}}{\partial \xi^\alpha} \cdot \widehat{\mathbf{g}}_\alpha = \widehat{\text{grad}}\{\bullet\} : \widehat{\mathbf{i}}$ $\widehat{\det}\{\bullet\} = \frac{ [\{\bullet\} \cdot \widehat{\mathbf{g}}_1] \times [\{\bullet\} \cdot \widehat{\mathbf{g}}_2] }{ \widehat{\mathbf{g}}_1 \times \widehat{\mathbf{g}}_2 }$ $\widehat{\mathbf{g}}_\alpha = \widehat{\mathbf{g}}_{\alpha\beta} \widehat{\mathbf{g}}^\beta \quad , \quad \widehat{\mathbf{g}}_{\alpha\beta} = \widehat{\mathbf{g}}_\alpha \cdot \widehat{\mathbf{g}}_\beta \quad , \quad \widehat{\mathbf{g}}^\alpha = \widehat{\mathbf{g}}^{\alpha\beta} \widehat{\mathbf{g}}_\beta \quad , \quad \widehat{\mathbf{g}}^{\alpha\beta} = \widehat{\mathbf{g}}^\alpha \cdot \widehat{\mathbf{g}}^\beta \quad , \quad [\widehat{\mathbf{g}}_{\alpha\beta}] = [\widehat{\mathbf{g}}^{\alpha\beta}]^{-1} \quad , \quad \widehat{\mathbf{g}} = \ \widehat{\mathbf{g}}_{\alpha\beta}\ $ $\widehat{\mathbf{g}} : \text{surface permutation tensor} \quad , \quad \widehat{\mathbf{g}} = \widehat{\mathbf{g}}_{\rho\sigma} \widehat{\mathbf{g}}^\rho \otimes \widehat{\mathbf{g}}^\sigma \otimes \mathbf{g}^3 = \widehat{\mathbf{g}}^{\rho\sigma} \widehat{\mathbf{g}}_\rho \otimes \widehat{\mathbf{g}}_\sigma \otimes \mathbf{g}_3 \quad , \quad \widehat{\mathbf{g}}_{\rho\sigma} = \widehat{\mathbf{g}}^{\rho\sigma} \widehat{\mathbf{g}} = \sqrt{\widehat{\mathbf{g}}} \widehat{\mathbf{e}}_{\rho\sigma}$ $\widehat{\mathbf{e}}_{\rho\sigma} = \begin{cases} 1 & \text{if } \rho\sigma \text{ is } 12 \\ -1 & \text{if } \rho\sigma \text{ is } 21 \\ 0 & \text{otherwise} \end{cases} \quad , \quad \widehat{\mathbf{g}}_{\rho\sigma} = \ [\widehat{\mathbf{g}}_\rho \times \widehat{\mathbf{g}}_\sigma]\ = \sqrt{\widehat{\mathbf{g}}} \widehat{\mathbf{e}}_{\rho\sigma} \quad , \quad \widehat{\mathbf{g}}^{\rho\sigma} = \ [\widehat{\mathbf{g}}^\rho \times \widehat{\mathbf{g}}^\sigma]\ = [\sqrt{\widehat{\mathbf{g}}}]^{-1} \widehat{\mathbf{e}}_{\rho\sigma}$ $\widehat{\mathbf{u}} \times \widehat{\mathbf{v}} = [\widehat{\mathbf{u}} \otimes \widehat{\mathbf{v}}] : \widehat{\mathbf{g}} \quad , \quad \widehat{\mathbf{u}} \cdot \widehat{\mathbf{v}} = [\widehat{\mathbf{u}} \otimes \widehat{\mathbf{v}}] : \widehat{\mathbf{i}} \quad , \quad \widehat{\mathbf{i}} = \delta_\beta^\alpha \widehat{\mathbf{g}}_\alpha \otimes \widehat{\mathbf{g}}^\beta = \widehat{\mathbf{g}}_\alpha \otimes \widehat{\mathbf{g}}^\alpha = \widehat{\mathbf{g}}_1 \otimes \widehat{\mathbf{g}}^1 + \widehat{\mathbf{g}}_2 \otimes \widehat{\mathbf{g}}^2 = \mathbf{i} - \mathbf{n} \otimes \mathbf{n}$
--	----------------------------------------------------------------------------------------------------------------------------------------------------------------------------------------------------------------------------------------------------------------------------------------------------------------------------------------------------------------------------------------------------------------------------------------------------------------------------------------------------------------------------------------------------------------------------------------------------------------------------------------------------------------------------------------------------------------------------------------------------------------------------------------------------------------------------------------------------------------------------------------------------------------------------------------------------------------------------------------------------------------------------------------------------------------------------------------------------------------------------------------------------------------------------------------------------------------------------------------------------------------------------------------------------------------------------------------------------------------------------------------------------------------------------------------------------------------------------------------------------------------------------------------------------------------------------------------------------------------------------------------------------------------------------------------------------------------------------------------------------------------------------------------------------------------------------------------------------------------------------------------------------------------------------------------------------------------------------------------------------------------------------------------------------------------------------------------------------------------------------------------------------------------------------------------------------------------------------------------------------------------------------------------------------------------------------------------------------------------------------------------------------------------------------------------------------------------------------------------------------------------------------------------------------------------------------------------------------------------------------------------------------------------------------------------------------------------------------------------------------------------------------------------------------------------------------------------------------------------------------------------------------------------------------------------------------------------------------------------------------------------------------------------------------------------------------------------------------------------------------------------------------------------------------------------------------------------------------------------------------------------------------------------------------------------------------------------------------------------------------------------------------------------------------------------------------------------------------

Fig. 3 The surface curvature is negative if the surface curves away from the normal (*left*) and positive vice versa (*right*). A surface can, of course, have a positive curvature along one line and negative curvature along another e.g. a saddle, gyroid etc



$\widehat{\mathbf{k}} = -\widehat{\text{grad}} \mathbf{n}$. The (invariant) trace of the surface curvature tensor is defined as $\widehat{\mathbf{k}}$ and renders twice the mean curvature, i.e. $\widehat{\mathbf{k}} = \widehat{\mathbf{k}} : \widehat{\mathbf{i}} = -\widehat{\text{div}} \mathbf{n}$ and furthermore, $\widehat{\text{div}} \widehat{\mathbf{i}} = \widehat{\mathbf{k}} \mathbf{n}$. In the context of the well-known Young–Laplace equation, $\widehat{\mathbf{k}} = -[1/r_1 + 1/r_2]$ where r_1 and r_2 are the principal radii of curvature. The negative sign arises from the convention that the curvature is negative if the surface curves away from its normal, and that the radii of curvatures are always positive, see Fig. 3. In this sense both cylinders and spheres have constant negative mean curvatures. In the framework presented here, we do not calculate radii of curvature and the curvature sign is intrinsically taken into account. The (invariant) determinant of the curvature tensor $\widehat{\mathbf{k}}$ is denoted $\widehat{\eta}$ and is known as Gaussian curvature. Clearly, a cylinder has a (constant)

Gaussian curvature of zero and a sphere a constant positive Gaussian curvature. \square

Remark Superficial and tangential quantities Second-order tensors and vectors on the surface can be classified as superficial (in their tangent spaces) or tangential. Superficial second-order tensors on the surface possess the orthogonality property $\{\bullet\} \cdot \mathbf{n} = \mathbf{0}$. If the arbitrary quantity in the preceding relation is a vector, it is termed tangential. Tangential second-order tensors on the surface are superficial and also possess the property $\mathbf{n} \cdot \{\bullet\} = \mathbf{0}$. \square

Remark Surface divergence theorem Let $\widehat{\mathbf{u}}$ denote a surface vector field not necessarily tangent to the surface. The surface

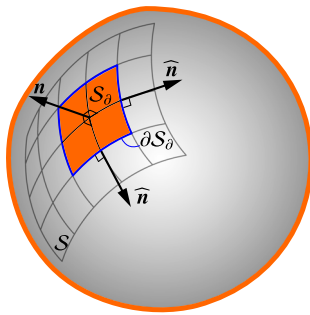


Fig. 4 A subsurface of the surface S is denoted as S_∂ with the boundary curve ∂S_∂ . The normal to the boundary curve and tangent to the surface is denoted \hat{n}

vector \hat{u} can be decomposed into its tangential and normal components as

$$\hat{u} = \hat{u}_\parallel + \hat{u}_\perp \quad \text{with} \quad \hat{u}_\parallel = \hat{u} \cdot \hat{i} \quad \text{and} \quad \hat{u}_\perp = \hat{u} \cdot [\hat{n} \otimes \hat{n}].$$

The surface divergence of \hat{u} is analogously decomposed as

$$\widehat{\text{div}} \hat{u} = \widehat{\text{div}} \hat{u}_\parallel + \widehat{\text{div}} \hat{u}_\perp = \widehat{\text{div}} \hat{u}_\parallel - \hat{\kappa} \hat{u} \cdot \hat{n}.$$

Let S_∂ denote a subsurface of the surface S with the boundary curve ∂S_∂ and \hat{n} denote the normal to the boundary curve and tangent to the surface as shown in Fig. 4. The surface divergence theorem, in analogy to the classical bulk divergence theorem, reads

$$\begin{aligned} \int_{S_\partial} \widehat{\text{div}} \hat{u}_\parallel \, da &= \int_{\partial S_\partial} \hat{u}_\parallel \cdot \hat{n} \, dl \quad \Rightarrow \quad \int_{S_\partial} \widehat{\text{div}} \hat{u} \, da \\ &= \int_{\partial S_\partial} \hat{u}_\parallel \cdot \hat{n} \, dl - \int_{S_\partial} \hat{\kappa} \hat{u} \cdot \hat{n} \, da. \end{aligned}$$

2.3 Problem definition

Consider a continuum body that takes the material configuration \mathcal{B}_0 at time t_0 and is mapped via the (bulk) non-

linear deformation map φ to the spatial configuration \mathcal{B}_t at any time $t > 0$ as shown in Fig. 5. The associated linear deformation map, i.e. the deformation gradient, is denoted as F and maps material line elements $dX \in T\mathcal{B}_0$ (tangent to \mathcal{B}_0) to spatial line elements $dx \in T\mathcal{B}_t$ via the relation $dx = F \cdot dX$. The bulk deformation gradient F is rank-sufficient and invertible. The bulk is understood as the collective placement of material particles $X \in \mathcal{B}_0$ and respectively $x \in \mathcal{B}_t$.

Let S_0 and S_t denote the surface of the continuum body in the material and spatial configurations, respectively. Material particles on the surface are denoted \hat{X} in the material configuration and are attached to the bulk, i.e. $\hat{X} = X|_{\partial\mathcal{B}_0}$. Thus $S_0 = \partial\mathcal{B}_0$. Furthermore, we assume that the surface is material in the sense that it is permanently attached to the substrate and therefore $S_t = \partial\mathcal{B}_t$ and $\hat{x} = x|_{\partial\mathcal{B}_t}$. This assumption implies that the motion of the surface $\hat{\varphi}$ is the restriction of the bulk motion φ to the surface, i.e. $\hat{\varphi} = \varphi|_{\partial\mathcal{B}_0}$. The material line elements on the surface in the material and spatial configurations are denoted by $d\hat{X} \in TS_0$ and $d\hat{x} \in TS_t$, respectively, and are related by $d\hat{x} = \hat{F} \cdot d\hat{X}$ where \hat{F} denotes the rank-deficient and thus non-invertible surface deformation gradient.

Remark Identity tensors in the material and spatial configurations In what follows the identity tensor is denoted as I or i and is understood as the conventional identity tensor in E^3 , i.e. its matrix representation would be a 3×3 matrix with 1 in the main diagonal entries and 0 elsewhere. Although these identity tensors are invariant and $i = I$, we use different letters to indicate explicitly which configuration they belong to. The reason for this can be better understood when considering the surface identity tensors. Let \hat{I} and \hat{i} denote the (rank deficient) surface identity tensors in E^3 in the material and spatial configurations, respectively. Due to their intrinsic structures $\hat{i} \neq \hat{I}$. Surface identity tensors should not be mistaken for the two-dimensional identities I_2 and i_2 in the material and spatial configurations, respectively. The two-

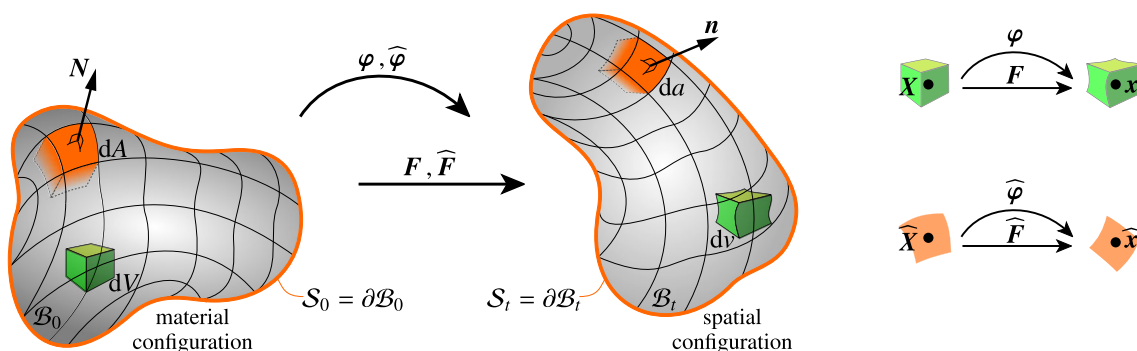


Fig. 5 The material and spatial configurations of a continuum body and its boundary and the associated deformation maps and deformation gradients

Table 3 Kinematics of the bulk

	$F = \frac{\partial \mathbf{x}}{\partial \mathbf{X}} = \text{Grad} \mathbf{x} \quad , \quad d\mathbf{x} = F \cdot d\mathbf{X}$ $[F] = \begin{bmatrix} \star & \star & \star \\ \star & \star & \star \\ \star & \star & \star \end{bmatrix}$ $f = \frac{\partial \mathbf{X}}{\partial \mathbf{x}} = \text{grad} \mathbf{X} \quad , \quad d\mathbf{X} = f \cdot d\mathbf{x}$
$J = \frac{\partial X}{\partial \xi} \quad , \quad dX = J \cdot d\xi$ $j = \frac{\partial x}{\partial \xi} \quad , \quad dx = j \cdot d\xi$ $J \cdot K = K \cdot J = I$ $dx = j \cdot d\xi = j \cdot K \cdot dX \Rightarrow F = j \cdot K$ $F = \frac{\partial \mathbf{x}}{\partial \mathbf{X}} = \frac{\partial \mathbf{x}}{\partial \xi} \cdot \frac{\partial \xi}{\partial \mathbf{X}} = \frac{\partial \mathbf{x}}{\partial \xi^i} \cdot \frac{\partial \xi^i}{\partial X} = \mathbf{g}_i \otimes \mathbf{G}^i$ $F = \mathbf{g}_1 \otimes \mathbf{G}^1 + \mathbf{g}_2 \otimes \mathbf{G}^2 + \mathbf{g}_3 \otimes \mathbf{G}^3$ $\text{Det} F = \frac{dv}{dV} = \frac{\mathbf{g}_1 \cdot [\mathbf{g}_2 \times \mathbf{g}_3]}{\mathbf{G}_1 \cdot [\mathbf{G}_2 \times \mathbf{G}_3]}$ $\text{Det} F = \frac{[F \cdot \mathbf{G}_1] \cdot [[F \cdot \mathbf{G}_2] \times [F \cdot \mathbf{G}_3]]}{\mathbf{G}_1 \cdot [\mathbf{G}_2 \times \mathbf{G}_3]}$ $f \cdot F = I \quad , \quad \det f = [\text{Det} F]^{-1} \quad , \quad F \cdot f = i$	$K = \frac{\partial \xi}{\partial X} \quad , \quad d\xi = K \cdot dX$ $k = \frac{\partial \xi}{\partial x} \quad , \quad d\xi = k \cdot dx$ $j \cdot k = k \cdot j = i$ $dX = J \cdot d\xi = J \cdot k \cdot dx \Rightarrow f = J \cdot k$ $f = \frac{\partial \mathbf{X}}{\partial \mathbf{x}} = \frac{\partial \mathbf{X}}{\partial \xi} \cdot \frac{\partial \xi}{\partial \mathbf{x}} = \frac{\partial \mathbf{X}}{\partial \xi^i} \cdot \frac{\partial \xi^i}{\partial x} = \mathbf{G}_i \otimes \mathbf{g}^i$ $f = \mathbf{G}_1 \otimes \mathbf{g}^1 + \mathbf{G}_2 \otimes \mathbf{g}^2 + \mathbf{G}_3 \otimes \mathbf{g}^3$ $\det f = \frac{dV}{dv} = \frac{\mathbf{G}_1 \cdot [\mathbf{G}_2 \times \mathbf{G}_3]}{\mathbf{g}_1 \cdot [\mathbf{g}_2 \times \mathbf{g}_3]}$ $\det f = \frac{[f \cdot \mathbf{g}_1] \cdot [[f \cdot \mathbf{g}_2] \times [f \cdot \mathbf{g}_3]]}{\mathbf{g}_1 \cdot [\mathbf{g}_2 \times \mathbf{g}_3]}$

dimensional identities $i_2 = I_2$ have full rank, in contrast to their surface counterparts, and their matrix representation is a 2×2 matrix with 1 in the diagonal entries and 0 elsewhere. \square

2.3.1 Kinematics of the bulk

A material line element in the bulk $d\mathbf{X} \in T\mathcal{B}_0$ is mapped to the corresponding spatial line element $d\mathbf{x} \in T\mathcal{B}_t$ via the deformation gradient F . The inverse of the deformation gradient is denoted as $f = F^{-1}$ and maps $d\mathbf{x}$ to $d\mathbf{X}$, i.e. $d\mathbf{X} = f \cdot d\mathbf{x}$. We define the natural configuration \mathcal{B}_\square as a reference configuration.² A material line element

$d\mathbf{X} \in T\mathcal{B}_0$ is mapped to the corresponding reference line element $d\xi \in T\mathcal{B}_\square$ via the linear map $K = J^{-1}$. Clearly J maps $d\xi$ to $d\mathbf{X}$ via $d\mathbf{X} = J \cdot d\xi$. Similar to the material configuration, the mappings between the spatial line element $d\mathbf{x}$ and the reference line element $d\xi \in T\mathcal{B}_\square$ are: $d\mathbf{x} = j \cdot d\xi$ and $d\xi = j^{-1} \cdot d\mathbf{x} = k \cdot d\mathbf{x}$. The deformation gradient F can be multiplicatively decomposed into the mapping from the material configuration to the reference configuration and from the reference configuration to the spatial configuration, i.e. $F = j \cdot J^{-1} = j \cdot K$ and analogously $f = J \cdot j^{-1} = J \cdot k$.

² Note that we distinguish between the material, spatial and natural configurations. A line element $d\mathbf{X}$ in the material configuration is mapped to

Footnote 2 continued

$d\mathbf{x}$ in the spatial configuration via the linear map F and to $d\xi$ in the natural (reference) configuration via K , see Table 3. The material, spatial and natural configurations on the surface are defined in a near-identical fashion to the bulk, see Table 4.

Table 4 Kinematics of the surface

	$\widehat{F} = \frac{\partial \widehat{x}}{\partial \widehat{X}} = \widehat{G} \widehat{\text{Grad}} \widehat{x}, \quad d\widehat{x} = \widehat{F} \cdot d\widehat{X}$ $[\widehat{F}] = \begin{bmatrix} \star & \star & 0 \\ \star & \star & 0 \\ \star & \star & 0 \end{bmatrix}$ $\widehat{f} = \frac{\partial \widehat{X}}{\partial \widehat{x}} = \widehat{\text{grad}} \widehat{X}, \quad d\widehat{X} = \widehat{f} \cdot d\widehat{x}$
$\widehat{J} = \frac{\partial \widehat{X}}{\partial \widehat{\xi}}, \quad d\widehat{X} = \widehat{J} \cdot d\widehat{\xi}$ $\widehat{j} = \frac{\partial \widehat{x}}{\partial \widehat{\xi}}, \quad d\widehat{x} = \widehat{j} \cdot d\widehat{\xi}$ $\widehat{J} \cdot \widehat{K} = \widehat{I}, \quad \widehat{K} \cdot \widehat{J} = I_2$ $d\widehat{x} = \widehat{j} \cdot d\widehat{\xi} = \widehat{j} \cdot \widehat{K} \cdot d\widehat{X} \Rightarrow \widehat{F} = \widehat{j} \cdot \widehat{K}$ $\widehat{F} = \frac{\partial \widehat{x}}{\partial \widehat{X}} = \frac{\partial \widehat{x}}{\partial \widehat{\xi}} \cdot \frac{\partial \widehat{\xi}}{\partial \widehat{X}} = \frac{\partial \widehat{x}}{\partial \widehat{\xi}^\alpha} \cdot \frac{\partial \widehat{\xi}^\alpha}{\partial \widehat{X}} = \widehat{g}_\alpha \otimes \widehat{G}^\alpha$ $\widehat{F} = \widehat{g}_1 \otimes \widehat{G}^1 + \widehat{g}_2 \otimes \widehat{G}^2$ $\widehat{\text{Det}} \widehat{F} = \frac{da}{dA} = \frac{ \widehat{g}_1 \times \widehat{g}_2 }{ \widehat{G}_1 \times \widehat{G}_2 } = \frac{ [\widehat{F} \cdot \widehat{G}_1] \times [\widehat{F} \cdot \widehat{G}_2] }{ \widehat{G}_1 \times \widehat{G}_2 }$	$\widehat{K} = \frac{\partial \widehat{\xi}}{\partial \widehat{X}}, \quad d\widehat{\xi} = \widehat{K} \cdot d\widehat{X}$ $\widehat{k} = \frac{\partial \widehat{\xi}}{\partial \widehat{x}}, \quad d\widehat{\xi} = \widehat{k} \cdot d\widehat{x}$ $\widehat{j} \cdot \widehat{k} = \widehat{i}, \quad \widehat{k} \cdot \widehat{j} = i_2$ $d\widehat{X} = \widehat{J} \cdot d\widehat{\xi} = \widehat{J} \cdot \widehat{k} \cdot d\widehat{x} \Rightarrow \widehat{f} = \widehat{J} \cdot \widehat{k}$ $\widehat{f} = \frac{\partial \widehat{X}}{\partial \widehat{x}} = \frac{\partial \widehat{X}}{\partial \widehat{\xi}} \cdot \frac{\partial \widehat{\xi}}{\partial \widehat{x}} = \frac{\partial \widehat{X}}{\partial \widehat{\xi}^\alpha} \cdot \frac{\partial \widehat{\xi}^\alpha}{\partial \widehat{x}} = \widehat{G}_\alpha \otimes \widehat{g}^\alpha$ $\widehat{f} = \widehat{G}_1 \otimes \widehat{g}^1 + \widehat{G}_2 \otimes \widehat{g}^2$ $\widehat{\text{det}} \widehat{f} = \frac{dA}{da} = \frac{ \widehat{G}_1 \times \widehat{G}_2 }{ \widehat{g}_1 \times \widehat{g}_2 } = \frac{ [\widehat{f} \cdot \widehat{g}_1] \times [\widehat{f} \cdot \widehat{g}_2] }{ \widehat{g}_1 \times \widehat{g}_2 }$
$\widehat{f} \cdot \widehat{F} = \widehat{I}, \quad \widehat{\text{det}} \widehat{f} = [\widehat{\text{Det}} \widehat{F}]^{-1}, \quad \widehat{F} \cdot \widehat{f} = \widehat{i}$	

Finally, an infinitesimal volume element in the material configuration dV is mapped to dv , the infinitesimal volume element in the spatial configuration, via the determinant of the deformation gradient, i.e. $dv = \text{Det} F dV$. The main concepts and definitions of the kinematics of the bulk are gathered in Table 3.

2.3.2 Kinematics of the surface

A material line element on the surface $d\widehat{X} \in TS_0$ is mapped to the corresponding spatial line element $d\widehat{x} \in TS_t$ via the surface deformation gradient \widehat{F} . The inverse of the rank-deficient surface deformation gradient is denoted by \widehat{f} and maps $d\widehat{x}$ to $d\widehat{X}$, i.e. $d\widehat{X} = \widehat{f} \cdot d\widehat{x}$. The relation of \widehat{F} to its

inverse \widehat{f} is defined as follows

$$\widehat{f} \cdot \widehat{F} = \widehat{I} \quad \text{and} \quad \widehat{F} \cdot \widehat{f} = \widehat{i}.$$

In an identical fashion to the bulk, the (surface) natural configuration S_\square is defined as a reference configuration. A material line element $d\widehat{X} \in TS_0$ is mapped to the corresponding reference line element $d\widehat{\xi} \in TS_\square$ via the linear map \widehat{K} . Clearly \widehat{J} maps $d\widehat{\xi}$ to $d\widehat{X}$ via $d\widehat{X} = \widehat{J} \cdot d\widehat{\xi}$. Similar to the material configuration, the spatial line element $d\widehat{x}$ and the reference line element $d\widehat{\xi}$ are related via the aforementioned mappings as follows: $d\widehat{x} = \widehat{j} \cdot d\widehat{\xi}$ and $d\widehat{\xi} = \widehat{k} \cdot d\widehat{x}$. The deformation gradient \widehat{F} can be multiplicatively decomposed into the mapping from the material configuration to the reference configuration and from the reference configuration to the spa-

Table 5 Governing equations

Strong form:

balance of linear momentum

balance of angular momentum

$$\text{Div} \mathbf{P} + \mathbf{b}_0^p = \mathbf{0}$$

,

$$\mathbf{F} \cdot \mathbf{P}^t = \mathbf{P} \cdot \mathbf{F}^t$$

in \mathcal{B}_0

$$\widehat{\text{Div}} \widehat{\mathbf{P}} + \widehat{\mathbf{b}}_0^p - \mathbf{P} \cdot \mathbf{N} = \mathbf{0}$$

,

$$\widehat{\mathbf{F}} \cdot \widehat{\mathbf{P}}^t = \widehat{\mathbf{P}} \cdot \widehat{\mathbf{F}}^t$$

on \mathcal{S}_0

Weak form:

$$\begin{aligned} \int_{\mathcal{B}_0} \mathbf{P} : \text{Grad} \delta \boldsymbol{\varphi} \, dV + \int_{\mathcal{S}_0} \widehat{\mathbf{P}} : \widehat{\text{Grad}} \delta \widehat{\boldsymbol{\varphi}} \, dA \\ - \int_{\mathcal{B}_0} \delta \boldsymbol{\varphi} \cdot \mathbf{b}_0^p \, dV - \int_{\mathcal{S}_0^N} \delta \widehat{\boldsymbol{\varphi}} \cdot \widehat{\mathbf{b}}_0^p \, dA = 0 \quad \forall \delta \boldsymbol{\varphi} \in \mathcal{H}_0^1(\mathcal{B}_0), \quad \forall \delta \widehat{\boldsymbol{\varphi}} \in \mathcal{H}_0^1(\mathcal{S}_0) \end{aligned}$$

tial configuration, i.e. $\widehat{\mathbf{F}} = \widehat{\mathbf{j}} \cdot \widehat{\mathbf{K}}$ and analogously $\widehat{\mathbf{f}} = \widehat{\mathbf{J}} \cdot \widehat{\mathbf{k}}$. An infinitesimal area element in the material configuration dA is mapped to da , the infinitesimal area element in the spatial configuration, via the surface determinant of the surface deformation gradient, i.e. $da = \widehat{\text{Det}} \widehat{\mathbf{F}} \, dA$. The main concepts and definitions of the kinematics of the surface are gathered in Table 4.

Remark Inverses of rank deficient tensors. The material Jacobian \mathbf{J} , spatial Jacobian \mathbf{j} and deformation gradient \mathbf{F} in the bulk are rank sufficient tensors and their inverses exist and are denoted as $\mathbf{K} = \mathbf{J}^{-1}$, $\mathbf{k} = \mathbf{j}^{-1}$ and $\mathbf{f} = \mathbf{F}^{-1}$, respectively. It is worth emphasizing that their surface counterparts are rank deficient and thus, non-invertible. Therefore, the notation $\widehat{\mathbf{J}}^{-1}$, $\widehat{\mathbf{j}}^{-1}$ and $\widehat{\mathbf{F}}^{-1}$ is intentionally not used in this manuscript. Nevertheless, $\widehat{\mathbf{K}}$, $\widehat{\mathbf{k}}$ and $\widehat{\mathbf{f}}$ can be understood as the generalized inverses of $\widehat{\mathbf{J}}$, $\widehat{\mathbf{j}}$ and $\widehat{\mathbf{F}}$, respectively, possessing the following properties:

$$\begin{aligned} \widehat{\mathbf{K}} \cdot \widehat{\mathbf{J}} = \mathbf{I}_2, \quad \widehat{\mathbf{J}} \cdot \widehat{\mathbf{K}} = \widehat{\mathbf{I}}, \quad \widehat{\mathbf{k}} \cdot \widehat{\mathbf{j}} = \mathbf{i}_2, \\ \widehat{\mathbf{j}} \cdot \widehat{\mathbf{k}} = \widehat{\mathbf{i}}, \quad \widehat{\mathbf{F}} \cdot \widehat{\mathbf{f}} = \widehat{\mathbf{I}}, \quad \widehat{\mathbf{f}} \cdot \widehat{\mathbf{F}} = \widehat{\mathbf{I}}. \end{aligned}$$

□

2.4 Governing equations

Let \mathbf{b}_0^p denote the prescribed body force field per unit volume in the material configuration. The surface traction is denoted by $\widehat{\mathbf{b}}_0^p$ and shall be understood as the prescribed surface force field per unit area in the material configuration. The strong form of the balance of linear and angular momentum in the bulk and on the surface are given in Table 5. For further details on the derivations of the governing equations, in both the material and spatial configurations, see [32].

The weak form of the linear momentum balances for the bulk and surface are obtained by first testing the respective strong form (from the left) with vector-valued (arbitrary) test functions $\delta \boldsymbol{\varphi} \in \mathcal{H}_0^1(\mathcal{B}_0)$ and $\delta \widehat{\boldsymbol{\varphi}} \in \mathcal{H}_0^1(\mathcal{S}_0)$, respectively. The result is then integrated over the corresponding domains in the material configurations, manipulated using the identities

$$\begin{aligned} \delta \boldsymbol{\varphi} \cdot \text{Div} \mathbf{P} &= \text{Div}(\delta \boldsymbol{\varphi} \cdot \mathbf{P}) - \mathbf{P} : \text{Grad} \delta \boldsymbol{\varphi} \quad \text{and} \\ \delta \widehat{\boldsymbol{\varphi}} \cdot \widehat{\text{Div}} \widehat{\mathbf{P}} &= \widehat{\text{Div}}(\delta \widehat{\boldsymbol{\varphi}} \cdot \widehat{\mathbf{P}}) - \widehat{\mathbf{P}} : \widehat{\text{Grad}} \delta \widehat{\boldsymbol{\varphi}}, \end{aligned}$$

which, together with the extended divergence theorems [28], the orthogonality properties of the surface Piola stress measure (which cause the integrals containing the curvature terms to vanish), and the kinematic condition $\delta \widehat{\boldsymbol{\varphi}} = \delta \boldsymbol{\varphi}|_{\partial \mathcal{B}_0}$, renders the weak form given in Table 5. Note that in writing the weak forms we distinguish between Neumann and Dirichlet-type boundary conditions. The domain \mathcal{S}_0^N denotes the Neumann part of the boundary \mathcal{S}_0 .

2.5 Constitutive relations

An isotropic hyperelastic material model is assumed for the constitutive response of the bulk (see Table 6). The free energy $\Psi = \Psi(\mathbf{F})$ is parametrized by the Lamé moduli λ and μ . An evaluation of the first Piola–Kirchhoff stress $\mathbf{P} := \partial \Psi / \partial \mathbf{F}$ and the Piola stress tangent $\mathbb{A} := \partial^2 \Psi / \partial \mathbf{F} \partial \mathbf{F}$ requires knowledge of the deformation gradient \mathbf{F} and its inverse \mathbf{f} .

The constitutive relation on the surface is chosen to mimic that in the bulk (see Table 7). In addition to a neo-Hookean type hyperelastic response, the surface free energy $\widehat{\Psi} = \widehat{\Psi}(\widehat{\mathbf{F}})$ accounts for surface tension via the parameter $\widehat{\gamma}$.

Table 6 Hyperelastic material model for the bulk

$J := \text{Det}\boldsymbol{F}$: Jacobian determinant	μ, λ	: Lamé constants
Free energy	$\Psi(\boldsymbol{F}) = \frac{1}{2} \lambda \ln^2 J + \frac{1}{2} \mu [\boldsymbol{F} : \boldsymbol{F} - 3 - 2 \ln J]$		
Piola stress	$\boldsymbol{P}(\boldsymbol{F}) = \frac{\partial \Psi}{\partial \boldsymbol{F}} = \lambda \ln J \boldsymbol{f}^t + \mu [\boldsymbol{F} - \boldsymbol{f}^t]$		
Piola stress tangent	$\mathbb{A}(\boldsymbol{F}) = \frac{\partial \boldsymbol{P}}{\partial \boldsymbol{F}} = \lambda [\boldsymbol{f}^t \otimes \boldsymbol{f}^t + \ln J \mathbb{D}] + \mu [\mathbb{I} - \mathbb{D}]$		
$\mathbb{D} := \frac{\partial \boldsymbol{f}^t}{\partial \boldsymbol{F}} = -\boldsymbol{f}^t \underline{\otimes} \boldsymbol{f} \qquad , \qquad \mathbb{I} := \frac{\partial \boldsymbol{F}}{\partial \boldsymbol{F}} = \boldsymbol{i} \overline{\otimes} \boldsymbol{I}$			

Table 7 Hyperelastic material model for the surface

$\widehat{J} := \widehat{\text{Det}} \widehat{\mathbf{F}}$: Surface Jacobian determinant	$\widehat{\mu}, \widehat{\lambda}$: Surface Lamé constants	$\widehat{\gamma}$: Surface tension
Surface Free energy	$\widehat{\Psi}(\widehat{\mathbf{F}}) = \frac{1}{2} \widehat{\lambda} \ln^2 \widehat{J} + \frac{1}{2} \widehat{\mu} [\widehat{\mathbf{F}} : \widehat{\mathbf{F}} - 2 - 2 \ln \widehat{J}] + \widehat{\gamma} \widehat{J}$				
Surface Piola stress	$\widehat{\mathbf{P}}(\widehat{\mathbf{F}}) = \frac{\partial \widehat{\Psi}}{\partial \widehat{\mathbf{F}}} = \widehat{\lambda} \ln \widehat{J} \widehat{\mathbf{f}}^t + \widehat{\mu} [\widehat{\mathbf{F}} - \widehat{\mathbf{f}}^t] + \widehat{\gamma} \widehat{J} \widehat{\mathbf{f}}^t$				
Surface Piola stress tangent	$\widehat{\mathbb{A}}(\widehat{\mathbf{F}}) = \frac{\partial \widehat{\mathbf{P}}}{\partial \widehat{\mathbf{F}}} = \widehat{\lambda} [\widehat{\mathbf{f}}^t \otimes \widehat{\mathbf{f}}^t + \ln \widehat{J} \widehat{\mathbb{D}}] + \widehat{\mu} [\widehat{\mathbb{I}} - \widehat{\mathbb{D}}] + \widehat{\gamma} \widehat{J} [\widehat{\mathbf{f}}^t \otimes \widehat{\mathbf{f}}^t + \widehat{\mathbb{D}}]$				
$\widehat{\mathbb{D}} := \frac{\partial \widehat{\mathbf{f}}^t}{\partial \widehat{\mathbf{F}}} = -\widehat{\mathbf{f}}^t \underline{\otimes} \widehat{\mathbf{f}} + [\mathbf{i} - \widehat{\mathbf{i}}] \underline{\otimes} [\widehat{\mathbf{f}} \cdot \widehat{\mathbf{f}}^t] \quad , \quad \widehat{\mathbb{I}} := \frac{\partial \widehat{\mathbf{F}}}{\partial \widehat{\mathbf{F}}} = \mathbf{i} \underline{\otimes} \widehat{\mathbf{I}}$					

The contribution of surface tension renders the surface free energy non-zero in the material configuration.

The assumption of isotropic and compressible neo-Hookean hyperelastic behaviour for the bulk and the surface is made only for simplicity. The framework is valid for more general constitutive equations. Introducing anisotropy or incompressibility into the constitutive response is straightforward. Nevertheless, it requires introducing extra numerical detail and further notation while providing little additional insight into the fundamental concepts.

The vast majority of models of surface elasticity presented in the literature are restricted to the linear theory. Care must be taken when linearizing the full theory. In particular, the surface linear strain tensor is not the symmetric part of the surface displacement gradient. The linear theory is given in Tables 8 and 9.

It should be emphasized that the surface material constants are independent of the bulk ones. These constants can be measured from atomistic calculations [10, 48]. Dingreville and Qu [13] developed a semi-analytic method to compute the surface elastic properties of crystalline materials. Moreover, a surface energy can be constructed using the surface Cauchy–Born hypothesis [39]. In [58] the surface parameters are obtained from ab initio calculations.

3 Aspects of the numerical implementation

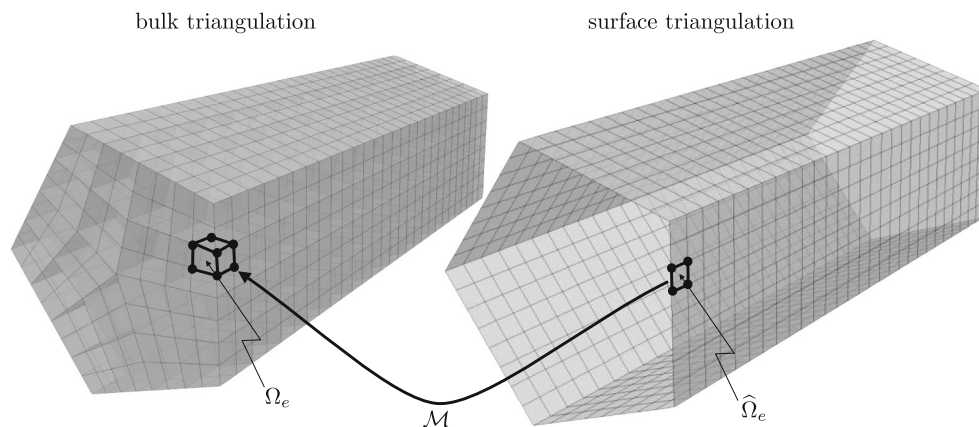
The finite element method is used to obtain approximate solutions to the governing equations presented in Table 5. The linearization of the governing equations and the construction of the resulting matrix problem have been pre-

Table 8 Linear infinitesimal strain material model for the bulk

$\text{Grad } \mathbf{u} = \mathbf{F} - \mathbf{I}$	\mathbf{u} : displacement vector	$\boldsymbol{\epsilon}$: infinitesimal strain tensor
$\boldsymbol{\epsilon} = [\text{Grad } \mathbf{u}]^{\text{sym}} = \mathbb{I}^{\text{sym}} : [\text{Grad } \mathbf{u}] = [\text{Grad } \mathbf{u}] + [\text{Grad } \mathbf{u}]^t$		
$\mathbb{I}^{\text{sym}} := \frac{1}{2} [\mathbf{I} \otimes \mathbf{I} + \mathbf{I} \otimes \mathbf{I}]$		
$\boldsymbol{\sigma} = \mathbb{E} : \boldsymbol{\epsilon}$, $\mathbb{E} = 3\lambda \mathbb{I}^{\text{vol}} + 2\mu \mathbb{I}^{\text{sym}}$		
$\boldsymbol{\sigma}$: linearized stress tensor	\mathbb{E} : 4 th order elastic moduli	$\mathbb{I}^{\text{vol}} := \frac{1}{3} \mathbf{I} \otimes \mathbf{I}$

Table 9 Linear infinitesimal strain material model for the surface

$\widehat{\text{Grad}} \widehat{\mathbf{u}} = \widehat{\mathbf{F}} - \widehat{\mathbf{I}}$	$\widehat{\mathbf{u}}$: surface displacement vector	$\widehat{\boldsymbol{\epsilon}}$: surface infinitesimal strain tensor
$\widehat{\boldsymbol{\epsilon}} = [\widehat{\text{Grad}} \widehat{\mathbf{u}}]^{\text{sym}} = \widehat{\mathbb{I}}^{\text{sym}} : [\widehat{\text{Grad}} \widehat{\mathbf{u}}] \neq [\widehat{\text{Grad}} \widehat{\mathbf{u}}] + [\widehat{\text{Grad}} \widehat{\mathbf{u}}]^t$		
$\widehat{\mathbb{I}}^{\text{sym}} := \frac{1}{2} [\widehat{\mathbf{I}} \otimes \widehat{\mathbf{I}} + \widehat{\mathbf{I}} \otimes \widehat{\mathbf{I}}]$		
$\widehat{\boldsymbol{\sigma}} = \widehat{\mathbb{E}} : \widehat{\boldsymbol{\epsilon}} + \widehat{\gamma} \widehat{\mathbf{I}} + \widehat{\gamma} \widehat{\text{Grad}} \widehat{\mathbf{u}}$, $\widehat{\mathbb{E}} = 2[\widehat{\lambda} + \widehat{\gamma}] \mathbb{I}^{\text{vol}} + 2[\widehat{\mu} - \widehat{\gamma}] \mathbb{I}^{\text{sym}}$		
$\widehat{\boldsymbol{\sigma}}$: linearized surface stress tensor	$\widehat{\mathbb{E}}$: 4 th order surface elastic moduli	$\mathbb{I}^{\text{vol}} := \frac{1}{2} \widehat{\mathbf{I}} \otimes \widehat{\mathbf{I}}$

**Fig. 6** Discretization of the bulk (a nanowire) and the surface into elements

sented in [31]. The complete documented source code and details of an efficient numerical implementation which mimics the framework presented here (developed using the open source finite element library `deal.II` [3,4]) are available in a companion paper [36]. The implementation uses various `deal.II` routines developed for the solution of partial differential equations on curved manifolds (see e.g. [11,23]). This set of routines is referred to as *codimension one* in `deal.II` terminology. The *codimension one* routines greatly simplify the construction of the approximations

to the various surface operators. For example, one can obtain directly the value of the surface gradient operators at the quadrature points of the surface mesh. The surface mesh is a two-dimensional manifold embedded in the surrounding three-dimensional space and is extracted directly from the bulk mesh (see Fig. 6). Elements in the bulk and on the surface are denoted Ω_e and $\widehat{\Omega}_e$, respectively. The contribution from the bulk to the global tangent matrix in the matrix problem is obtained by looping over all the bulk elements Ω_e , assembling the element contribution, and then

Table 10 Key step to evaluate the constitutive relation at the level of a quadrature point in the bulk

Preprocessing:

- Record the nodal coordinates, denoted \mathbf{X}^I and \mathbf{x}^I in the material and spatial configurations, respectively, corresponding to each node I .

At each quadrature point ξ in the element Ω_e :

- Interpolate the coordinates corresponding to ξ using the element shape functions $N^I(\xi)$:

$$\mathbf{X}(\xi) = \sum_I N^I(\xi) \mathbf{X}^I, \quad \mathbf{x}(\xi) = \sum_I N^I(\xi) \mathbf{x}^I.$$

- Calculate covariant bases in the material and spatial configurations (\mathbf{G}_i and \mathbf{g}_i):

$$\mathbf{G}_i = \sum_I \frac{\partial N^I}{\partial \xi^i} \mathbf{X}^I, \quad \mathbf{g}_i = \sum_I \frac{\partial N^I}{\partial \xi^i} \mathbf{x}^I.$$

- Calculate covariant metrics (matrices) in the material and spatial configurations ($[G_{ij}]$ and $[g_{ij}]$):

$$\mathbf{G}_{ij} = \mathbf{G}_i \cdot \mathbf{G}_j, \quad [G_{ij}] = \begin{bmatrix} G_{11} & G_{12} & G_{13} \\ G_{21} & G_{22} & G_{23} \\ G_{31} & G_{32} & G_{33} \end{bmatrix}, \quad \mathbf{g}_{ij} = \mathbf{g}_i \cdot \mathbf{g}_j, \quad [g_{ij}] = \begin{bmatrix} g_{11} & g_{12} & g_{13} \\ g_{21} & g_{22} & g_{23} \\ g_{31} & g_{32} & g_{33} \end{bmatrix}.$$

- Calculate contravariant metrics in the material and spatial configurations ($[G^{ij}]$ and $[g^{ij}]$):

$$[G^{ij}] = [G_{ij}]^{-1}, \quad [g^{ij}] = [g_{ij}]^{-1}.$$

- Calculate contravariant bases in the material and spatial configurations (\mathbf{G}^i and \mathbf{g}^i):

$$\mathbf{G}^i = G^{ij} \cdot \mathbf{G}_j, \quad \mathbf{g}^i = g^{ij} \cdot \mathbf{g}_j.$$

- Calculate kinematic quantities required to evaluate the constitutive relations:

$$\begin{aligned} \mathbf{F} &= \mathbf{g}_i \otimes \mathbf{G}^i, & \mathbf{F}^t &= \mathbf{G}^i \otimes \mathbf{g}_i, & \mathbf{I} &= \mathbf{G}_i \otimes \mathbf{G}^i, & \mathbf{C} &= \mathbf{F}^t \cdot \mathbf{F} = g_{ij} \mathbf{G}^i \otimes \mathbf{G}^j \\ \mathbf{f} &= \mathbf{G}_i \otimes \mathbf{g}^i, & \mathbf{f}^t &= \mathbf{g}^i \otimes \mathbf{G}_i, & \mathbf{i} &= \mathbf{g}_i \otimes \mathbf{g}^i, & \mathbf{b} &= \mathbf{F} \cdot \mathbf{F}^t = G^{ij} \mathbf{g}_i \otimes \mathbf{g}_j. \end{aligned}$$

adding this to the global tangent matrix. The contribution from the surface is obtained in a similar way. A loop is performed over all surface elements $\widehat{\Omega}_e$ and the tangent contribution calculated. A map between the degrees of freedom on the surface and the bulk, denoted \mathcal{M} , is then used to add the surface element's contribution to the global tangent matrix.

A key step in the numerical solution procedure is the evaluation of the constitutive relations. From Tables 10 and 11, it is clear that in order to evaluate the constitutive relations, an efficient procedure to determine the deformation gradient and its inverse at the level of the quadrature point within an element is required. An efficient formulation is obtained by adopting the same methodology for both the bulk and the surface. The key steps to evaluate

the hyperelastic constitutive relations at the level of a typical quadrature point within an element in a finite element scheme using this unified approach are provided in Tables 10 and 11.

4 Numerical results

The objective of the current section is to elucidate key features of the formulation using three example problems. The first example illustrates neo-Hookean type surface effects in a nanowire undergoing significant tensile extension. Surface tension is omitted. The second example of a liquid bridge explores the role of isotropic surface tension. The third example illustrates neo-Hookean type sur-

Table 11 Key step to evaluate the constitutive relation at the level of the quadrature point on the surface

Preprocessing:

- Record the nodal coordinates in the material and spatial configurations, denoted \widehat{X}^I and \widehat{x}^I , respectively.

At each quadrature point $\widehat{\xi}$ in the element $\widehat{\Omega}_e$:

- Interpolate the coordinates corresponding to $\widehat{\xi}$ using the element shape functions $\widehat{N}^I(\widehat{\xi})$:

$$\widehat{X}(\widehat{\xi}) = \sum_I \widehat{N}^I(\widehat{\xi}) \widehat{X}^I, \quad \widehat{x}(\widehat{\xi}) = \sum_I \widehat{N}^I(\widehat{\xi}) \widehat{x}^I.$$

- Calculate covariant bases in the material and spatial configurations (\widehat{G}_α and \widehat{g}_α):

$$\widehat{G}_\alpha = \sum_I \frac{\partial \widehat{N}^I}{\partial \xi^\alpha} \widehat{X}^I, \quad \widehat{g}_\alpha = \sum_I \frac{\partial \widehat{N}^I}{\partial \xi^\alpha} \widehat{x}^I.$$

- Calculate covariant metrics (matrices) in the material and spatial configurations ($[\widehat{G}_{\alpha\beta}]$ and $[\widehat{g}_{\alpha\beta}]$):

$$\widehat{G}_{\alpha\beta} = \widehat{G}_\alpha \cdot \widehat{G}_\beta, \quad [\widehat{G}_{\alpha\beta}] = \begin{bmatrix} \widehat{G}_{11} & \widehat{G}_{12} \\ \widehat{G}_{21} & \widehat{G}_{22} \end{bmatrix}, \quad \widehat{g}_{\alpha\beta} = \widehat{g}_\alpha \cdot \widehat{g}_\beta, \quad [\widehat{g}_{\alpha\beta}] = \begin{bmatrix} \widehat{g}_{11} & \widehat{g}_{12} \\ \widehat{g}_{21} & \widehat{g}_{22} \end{bmatrix}.$$

- Calculate contravariant metrics in the material and spatial configurations ($[\widehat{G}^{\alpha\beta}]$ and $[\widehat{g}^{\alpha\beta}]$):

$$[\widehat{G}^{\alpha\beta}] = [\widehat{G}_{\alpha\beta}]^{-1}, \quad [\widehat{g}^{\alpha\beta}] = [\widehat{g}_{\alpha\beta}]^{-1}.$$

- Calculate contravariant bases in the material and spatial configurations (\widehat{G}^α and \widehat{g}^α):

$$\widehat{G}^\alpha = \widehat{G}^{\alpha\beta} \cdot \widehat{G}_\beta, \quad \widehat{g}^\alpha = \widehat{g}^{\alpha\beta} \cdot \widehat{g}_\beta.$$

- Calculate kinematic quantities required to evaluate the constitutive relations:

$$\begin{aligned} \widehat{F} &= \widehat{g}_\alpha \otimes \widehat{G}^\alpha, & \widehat{F}^t &= \widehat{G}^\alpha \otimes \widehat{g}_\alpha, & \widehat{I} &= \widehat{G}_\alpha \otimes \widehat{G}^\alpha, & \widehat{C} &= \widehat{F}^t \cdot \widehat{F} = \widehat{g}_{\alpha\beta} \widehat{G}^\alpha \otimes \widehat{G}^\beta \\ \widehat{f} &= \widehat{g}_\alpha \otimes \widehat{g}^\alpha, & \widehat{f}^t &= \widehat{g}^\alpha \otimes \widehat{g}_\alpha, & \widehat{i} &= \widehat{g}_\alpha \otimes \widehat{g}^\alpha, & \widehat{b} &= \widehat{F} \cdot \widehat{F}^t = \widehat{G}^{\alpha\beta} \widehat{g}_\alpha \otimes \widehat{g}_\beta \end{aligned}$$

- Perform consistency check:

$$N = \frac{\widehat{G}_1 \times \widehat{G}_2}{|\widehat{G}_1 \times \widehat{G}_2|} \Rightarrow \widehat{I} = I - N \otimes N, \quad \widehat{F} = F \cdot \widehat{I}, \quad n = \frac{\widehat{g}_1 \times \widehat{g}_2}{|\widehat{g}_1 \times \widehat{g}_2|} \Rightarrow \widehat{i} = i - n \otimes n, \quad \widehat{f} = f \cdot \widehat{i}.$$

face effects in a nanoscale plate with a realistic rough surface. The constitutive relations are given in Tables 6 and 7.

Trilinear and bilinear hexahedral and quadrilateral elements are used in the bulk and on the surface, respectively. The linearized matrix problem is solved using the conjugate gradient method with Jacobi preconditioning. The finite element formulation is implemented within the total Lagrangian framework. A Bubnov–Galerkin approach is adopted; for

more details on the finite element scheme see the companion paper [36].

4.1 Nanowire: neo-Hookean boundary potential

Surface elasticity theory has been used to describe successfully surface effects in nanowires (see e.g. [57, 58]). Consider the benchmark example shown in Fig. 7. The front and back pentagonal faces are prevented from displacing in the X and

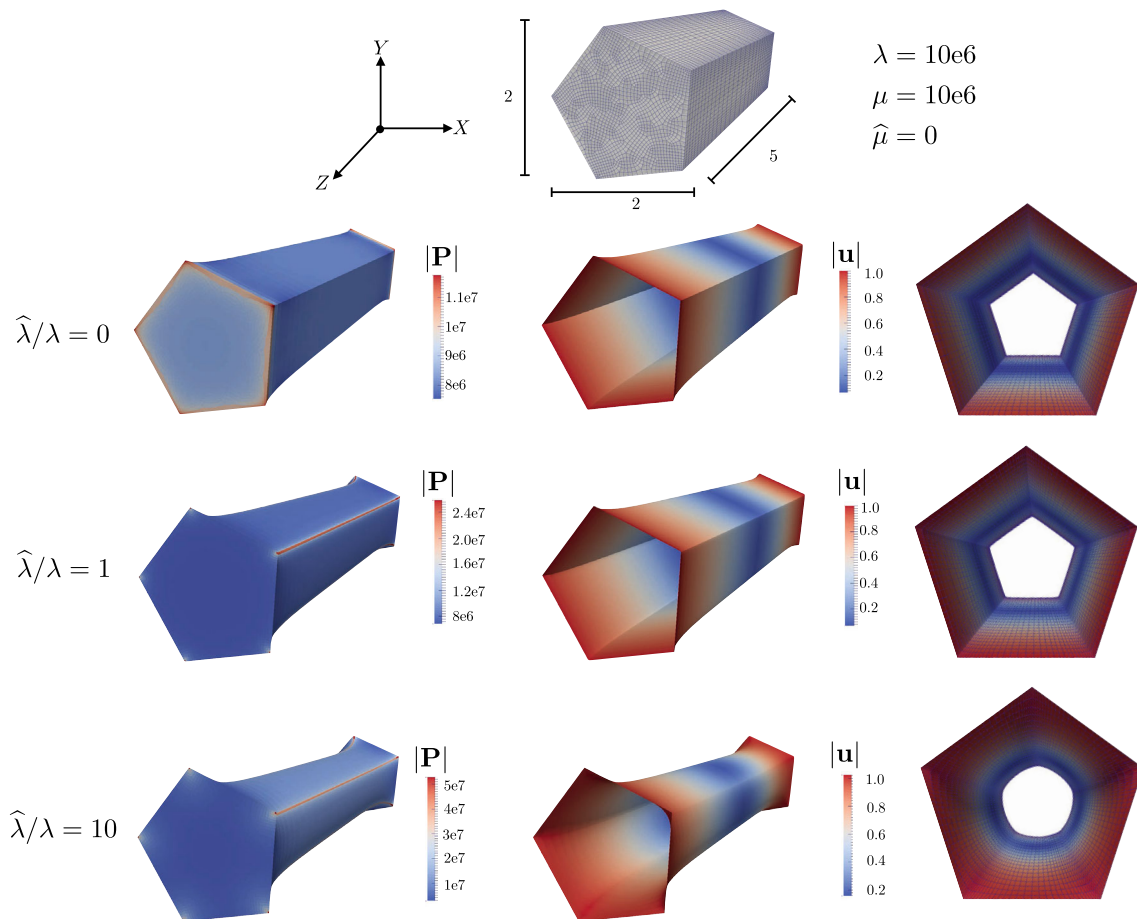


Fig. 7 The triangulation and material configuration for the nanowire. The fixed material properties are given. The final spatial configuration of the bulk and the surface for three different ratios of $\hat{\lambda}/\lambda$ are shown

Y directions. The wire is extended in the Z -direction by an amount of 2 (i.e. 40 % of the original length). The unconstrained surfaces on the side of the wire are energetic, i.e. they possess their own surface energy.

The triangulation of the bulk is more refined at the intersection of the faces on the surface and towards the front and back faces. This is done to better resolve the expected stress concentrations. The bulk and surface are discretized into 45 570 and 4500 elements, respectively. The prescribed deformation is applied uniformly in 10 steps.

The Lamé parameters in the bulk are fixed at the values given in Fig. 7. Similarly, the neo-Hookean energetic surface is characterized by the surface Lamé parameters $\hat{\lambda}$ and $\hat{\mu}$ (for a detailed discussion on surface material parameters see [29, 32]). The surface shear modulus $\hat{\mu}$ is set to zero and the ratio $\hat{\lambda}/\lambda$ varied.

The response in the absence of a surface energy is obtained by choosing $\hat{\lambda}/\lambda = 0$ and is shown in Fig. 7. The stress in the bulk concentrates at the corners on the front and back faces. The initially pentagonal cross section reduces almost uniformly in size along the length.

A surface energy is then assigned to the external surface. The stress in the bulk \mathbf{P} concentrates along the lines of intersection of the planes that form the external surface as the value of $\hat{\lambda}$ increases. Increasing the surface energy causes the resulting deformed cross section to tend to circular, thus increasing the stress in the bulk in regions where the surface is not smooth. The norm of the stress in the bulk $|\mathbf{P}|$ evaluated on the surface is compared to the norm of the surface stress $|\hat{\mathbf{P}}|$ in Fig. 8 for a ratio of $\hat{\lambda}/\lambda = 1$.

4.2 Liquid bridge: isotropic surface tension effects

A liquid bridge is a thin film suspended between two rigid circular side walls, as depicted in Fig. 9. Surface tension acts in the material configuration to deform the surface so as to minimize its surface area. The bulk and surface triangulation contains 36,226 and 18,290 elements, respectively.

In order to model the liquid bridge using the approach adopted here, a bulk must be present. The bulk is a thin-walled cylinder (with a thickness of 0.1) composed of a neo-Hookean material with Lamé parameters of $\lambda = 0$ and $\mu =$

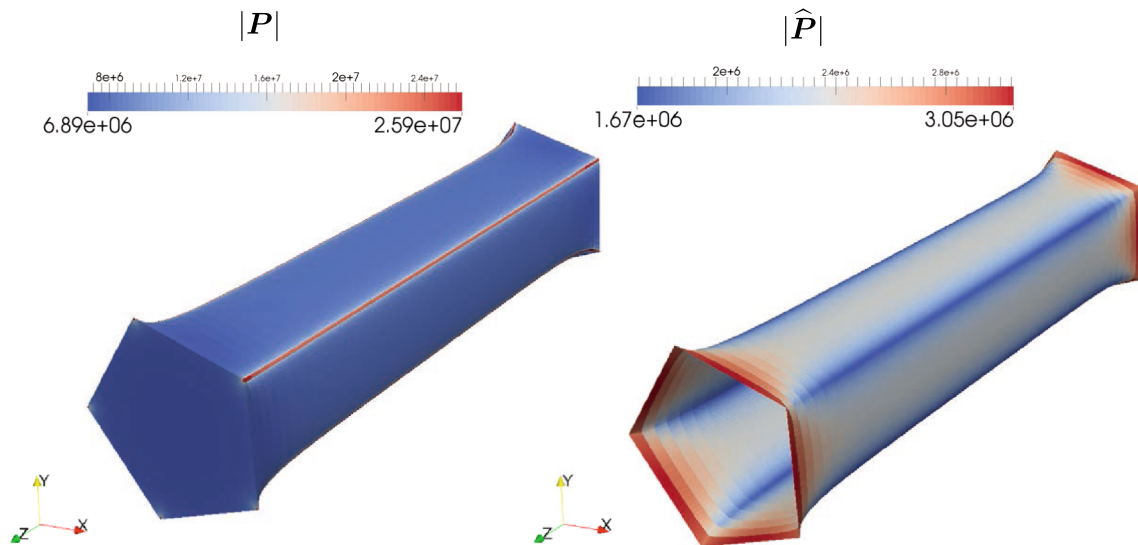


Fig. 8 Comparison of $|P|$ and $|\hat{P}|$ for the ratio of $\hat{\lambda}/\lambda = 1$

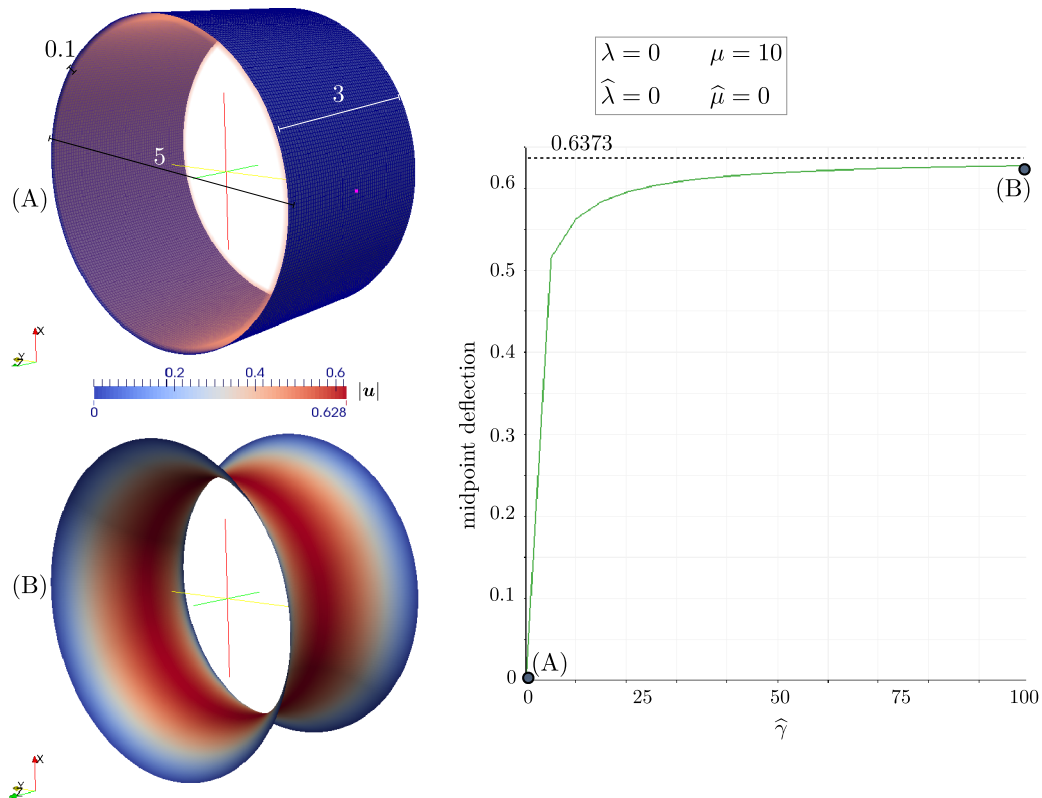


Fig. 9 The liquid bridge in the material configuration and the deformed state corresponding $\hat{\gamma} = 100$. The deflection of a point on the centre line of the surface versus the value of $\hat{\gamma}$ is shown

10, and is enclosed by the energetic surface. Note that the surface free energy is non-zero in the reference configuration.

The surface free energy, i.e. $\hat{\gamma}$, is linearly increased over 20 equal steps to a value of 100 and the displacement of a point on the middle of the surface monitored. The deflec-

tion of the monitored point on the surface for varying $\hat{\gamma}$ is shown in Fig. 9. The configuration at two selected values of $\hat{\gamma}$ is also shown. The majority of the deformation occurs for $\hat{\gamma} < 10$. Thereafter, as $\hat{\gamma}$ increases so the midpoint deflection converges to the analytical solution of 0.6373 see [31].

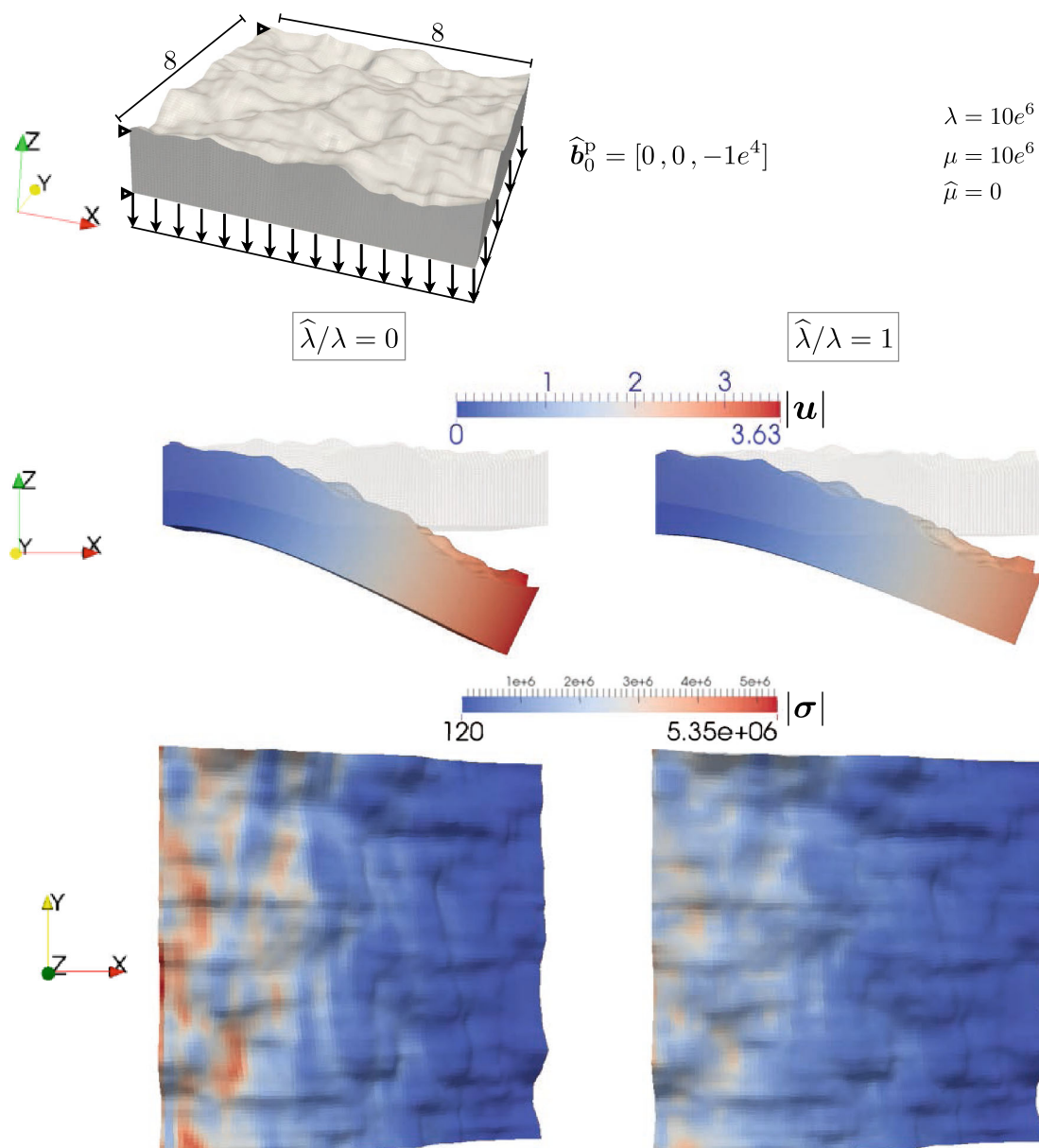


Fig. 10 The triangulation and material configuration for the cantilever plate. The fixed material properties are given. The final spatial configuration of the bulk for two different ratios of $\hat{\lambda}/\lambda$ are shown. The magnitude of the displacement \mathbf{u} and the Frobenius norm of the Cauchy stress $\boldsymbol{\sigma}$ fields are plotted

4.3 Bending of a nanoscale plate with a rough surface

Surface roughness can have a significant, and often complex, influence on the response of nanoscale objects (see e.g. [52] and the references therein). Consider the cantilever plate shown in Fig. 10. The rough upper surface is assumed energetic. All other surfaces are planar and standard. The Lamé parameters in the bulk are fixed at the values given in Fig. 10. The surface shear modulus $\hat{\mu}$ is set to zero and the ratio $\hat{\lambda}/\lambda$ varied. The left edge of the plate is fully fixed and a prescribed surface traction of $\hat{\mathbf{b}}_0^p = [0, 0, -1e^4]$ is imposed incrementally (in 10 uniform steps) on the lower face. The

bulk and surface triangulation contains 250 000 and 10 000 elements, respectively. The profile of the upper surface was produced using an open source rough surface generation tool [7].³

The response of the plate to the loading for $\hat{\lambda}/\lambda = 0$ and $\hat{\lambda}/\lambda = 1$ are compared in Fig. 10. The plate with the energetic rough surface deforms less.

³ The routine used, *rsgene2D*, produces a Gaussian height distribution with an exponential auto-covariance. The input parameters were 100 divisions, a surface length of 2, a root mean square height of 0.05, and an (isotropic) correlation length of 0.25.

The example of the cantilever plate with the rough surface provides a good test of the robustness of the numerical implementation. The Newton scheme exhibited the quadratic convergence associated with a consistently derived tangent. Furthermore, the example demonstrates the effectiveness of the curvilinear coordinate framework to describe complex surface geometries.

5 Discussion and conclusions

A finite element methodology based on describing the surface and bulk behaviour using a curvilinear coordinate framework has been presented. The advantage of such a methodology is clear for problems in surface elasticity: the computation of the surface quantities is straightforward. The key steps required to evaluate the constitutive relations at the level of the quadrature point have also been presented. The implementation of the formulation within an open source finite element library is discussed in a companion contribution [36]. The use of adaptive finite element methods and the development of a distributed parallel solution strategy, necessary when modelling realistic and complex geometries, is the focus of ongoing research.

References

- Agrawal R, Peng B, Gdoutos EE, Espinosa HD (2008) Elasticity size effects in ZnO nanowires: a combined experimental–computational approach. *Nano Lett* 8(11):3668–3674
- Altenbach H, Eremeyev V (2011) On the shell theory on the nanoscale with surface stresses. *Int J Eng Sci* 49(12):1294–1301
- Bangerth W, Hartmann R, Kanschat G (2007) deal.II: A general purpose object oriented finite element library. *ACM Trans Math Softw* 33(4):24
- Bangerth W, Heister T, Kanschat G et al (2013) deal.II Differential equations analysis library, Technical Reference <http://www.dealii.org>
- Benveniste Y, Berdichevsky O (2010) On two models of arbitrarily curved three-dimensional thin interphases in elasticity. *Int J Solids Struct* 47(1415):1899–1915
- Benveniste Y, Miloh T (2001) Imperfect soft and stiff interfaces in two-dimensional elasticity. *Mech Mater* 33(6):309–323
- Bergström D (2013) <http://www.mysimlabs.com/surface/generation.html>
- Cammarata RC (1994) Surface and interface stress effects in thin films. *Prog Surf Sci* 46(1):1–38
- Ciarlet PG (2005) An introduction to differential geometry with applications to elasticity. *J Elast* 78:1–215
- Davydov D, Javili A, Steinmann P (2013) On molecular statics and surface-enhanced continuum modeling of nano-structures. *Comput Mater Sci* 69:510–519
- DeSimone A, Heltai L, Manigrasso C (2009) Tools for the solution of pdes defined on curved manifolds with deal.II. <http://www.dealii.org/7.3.0/reports/codimension-one/desimone-heltai-manigrasso.pdf>
- Dettmer W, Perić D (2006) A computational framework for free surface fluid flows accounting for surface tension. *Comput Methods Appl Mech Eng* 195(23–24):3038–3071
- Dingreville R, Qu J (2007) A semi-analytical method to compute surface elastic properties. *Acta Mater* 55(1):141–147
- Dingreville R, Qu J, Cherkaoui M (2005) Surface free energy and its effect on the elastic behavior of nano-sized particles, wires and films. *J Mech Phys Solids* 53(8):1827–1854
- Duan H, Wang J, Karihaloo B (2009) Theory of elasticity at the nonoscale. *Adv Appl Mech* 42:1–68
- Duan HL, Karihaloo BL (2007) Effective thermal conductivities of heterogeneous media containing multiple imperfectly bonded inclusions. *Phys Rev B* 75:64206
- Duan HL, Wang J, Huang ZP, Karihaloo BL (2005) Eshelby formalism for nano-inhomogeneities. *Proc R Soc A* 461(2062):3335–3353
- Fischer FD, Svoboda J (2010) Stresses in hollow nanoparticles. *Sci Direct* 47:2799–2805
- Green AE, Zerna W (1968) Theoretical elasticity. Oxford University Press, Oxford
- Gu ST, He Q-C (2011) Interfacial discontinuity relations for coupled multifield phenomena and their application to the modeling of thin interphases as imperfect interfaces. *J Mech Phys Solids* 59(7):1413–1426
- Gurtin ME, Murdoch AI (1975) A continuum theory of elastic material surfaces. *Arch Ration Mech Anal* 57(4):291–323
- He J, Lilley CM (2008) Surface effect on the elastic behavior of static bending nanowires. *Nano Lett* 8(7):1798–1802
- Heltai L (2008) On the stability of the finite element immersed boundary method. *Comput Struct* 86(7–8):598–617
- Herring C (1951) Some theorems on the free energies of crystal surfaces. *Phys Rev* 82(1):87–93
- Huang Z, Sun L (2007) Size-dependent effective properties of a heterogeneous material with interface energy effect: from finite deformation theory to infinitesimal strain analysis. *Acta Mech* 190:151–163
- Hung Z, Wang J (2006) A theory of hyperelasticity of multi-phase media with surface/interface energy effect. *Acta Mech* 182:195–210
- Itskov M (2007) Tensor algebra and tensor analysis for engineers. Springer, Berlin
- Javili A, McBride A, Steinmann P (2013) Thermomechanics of solids with lower-dimensional energetics: on the importance of surface, interface and curve structures at the nanoscale. A unifying review. *Appl Mech Rev* 65(1):010802
- Javili A, McBride A, Steinmann P, Reddy BD (2012) Relationships between the admissible range of surface material parameters and stability of linearly elastic bodies. *Philos Mag* 92:3540–3563
- Javili A, Steinmann P (2009) A finite element framework for continua with boundary energies. Part I: the two-dimensional case. *Comput Methods Appl Mech Eng* 198(27–29):2198–2208
- Javili A, Steinmann P (2010a) A finite element framework for continua with boundary energies. Part II: the three-dimensional case. *Comput Methods Appl Mech Eng* 199(9–12):755–765
- Javili A, Steinmann P (2010b) On thermomechanical solids with boundary structures. *Int J Solids Struct* 47(24):3245–3253
- Javili A, Steinmann P (2011) A finite element framework for continua with boundary energies. Part III: the thermomechanical case. *Comput Methods Appl Mech Eng* 200(21–22):1963–1977
- Kreyszig E (1991) Differential geometry. Dover Publications, New York
- Levitass VI (2013) Thermodynamically consistent phase field approach to phase transformations with interface stresses. *Acta Mater* 61:4305–4319
- McBride A, Javili A (2013) An efficient finite element implementation for problems in surface elasticity.

37. Miller RE, Shenoy VB (2000) Size-dependent elastic properties of nanosized structural elements. *Nanotechnology* 11(3):139
38. Orowan E (1970) Surface energy and surface tension in solids and liquids. *Proc R Soc* 316:473–491
39. Park HS, Klein PA (2007) Surface Cauchy–Born analysis of surface stress effects on metallic nanowires. *Phys Rev B* 75(8):1–9
40. Park HS, Klein PA (2008) A Surface Cauchy–Born model for silicon nanostructures. *Comput Methods Appl Mech Eng* 197(41–42):3249–3260
41. Park HS, Klein PA, Wagner GJ (2006) A surface Cauchy–Born model for nanoscale materials. *Int J Numer Methods Eng* 68(10):1072–1095
42. Saksono PH, Perić D (2005) On finite element modelling of surface tension variational formulation and applications. Part I: quasistatic problems. *Comput Mech* 38(3):265–281
43. Scriven LE (1960) Dynamics of a fluid interface equation of motion for newtonian surface fluids. *Chem Eng Sci* 12(2):98–108
44. Scriven LE, Sternling CV (1960) The marangoni effects. *Nature* 187:186–188
45. Sharma P, Ganti S (2004) Size-dependent Eshelby’s tensor for embedded nano-inclusions incorporating surface/interface energies. *J Appl Mech* 71:663–671
46. Sharma P, Ganti S, Bhate N (2003) Effect of surfaces on the size-dependent elastic state of nano-inhomogeneities. *Appl Phys Lett* 82(4):535–537
47. Sharma P, Wheeler LT (2007) Size-dependent elastic state of ellipsoidal nano-inclusions incorporating surface/interface tension. *J Appl Mech* 74(3):447–454
48. Shenoy VB (2005) Atomistic calculations of elastic properties of metallic fcc crystal surfaces. *Phys Rev B* 71(9):1–11
49. Shuttleworth R (1950) The surface tension of solids. *Proc Phys Soc Sect A* 63(5):444–457
50. Steigmann DJ (2009) A concise derivation of membrane theory from three-dimensional nonlinear elasticity. *J Elast* 97:97–101
51. Sussmann C, Givoli D, Benveniste Y (2011) Combined asymptotic finite-element modeling of thin layers for scalar elliptic problems. *Comput Methods Appl Mech Eng* 200(4748):3255–3269
52. Wang Y, Weissmüller J, Duan HL (2010a) Mechanics of corrugated surfaces. *J Mech Phys Solids* 58:1552–1566
53. Wang Z-Q, Zhao Y-P, Huang Z-P (2010b) The effects of surface tension on the elastic properties of nano structures. *Int J Eng Sci* 48(2):140–150
54. Wei GW, Shouwen Y (2006) Finite element characterization of the size-dependent mechanical behaviour in nanosystems. *Nanotechnology* 17(4):1118–1122
55. Weissmüller J, Duan H-L, Farkas D (2010) Deformation of solids with nanoscale pores by the action of capillary forces. *Acta Mater* 58(1):1–13
56. Wriggers P (2008) *Nonlinear finite element methods*. Springer, Berlin
57. Yun G, Park HS (2009) Surface stress effects on the bending properties of fcc metal nanowires. *Phys Rev B* 79(19):32–35
58. Yvonnet J, Mitrushchenkov A, Chambaud G, He Q-C (2011) Finite element model of ionic nanowires with size-dependent mechanical properties determined by ab initio calculations. *Comput Methods Appl Mech Eng* 200(5–8):614–625
59. Yvonnet J, Quang HL, He Q-C (2008) An XFEM level set approach to modelling surface–interface effects and computing the size-dependent effective properties of nanocomposites. *Comput Mech* 42(1):119–131